High-Performance Reaction Wheel Optimization for Fine-Pointing Space Platforms: Minimizing Induced Vibration Effects on Jitter Performance plus Lessons Learned from Hubble Space Telescope for Current and Future Spacecraft Applications

Martin D. Hasha[*]

Abstract

The Hubble Space Telescope (HST) applies large-diameter optics (2.5-m primary mirror) for diffraction-limited resolution spanning an extended wavelength range (~100-2500 nm). Its Pointing Control System (PCS) Reaction Wheel Assemblies (RWAs), in the Support Systems Module (SSM), acquired an unprecedented set of high-sensitivity Induced Vibration (IV) data for 5 flight-certified RWAs: dwelling at set rotation rates. Focused on 4 key ratios, force and moment harmonic values (in 3 local principal directions) are extracted in the RWA operating range (0-3000 RPM). The IV test data, obtained under ambient lab conditions, are investigated in detail, evaluated, compiled, and curve-fitted; variational trends, core causes, and unforeseen anomalies are addressed. In aggregate, these values constitute a statistically-valid basis to quantify ground test-to-test variations and facilitate extrapolations to on-orbit conditions. Accumulated knowledge of bearing-rotor vibrational sources, corresponding harmonic contributions, and salient elements of IV key variability factors are discussed. An evolved methodology is presented for absolute assessments and relative comparisons of macro-level IV signal magnitude due to micro-level construction-assembly geometric details/imperfections stemming from both electrical drive and primary bearing design parameters. Based upon studies of same-size/similar-design momentum wheels' IV changes, upper estimates due to transitions from ground tests to orbital conditions are derived. Recommended HST RWA choices are discussed relative to system optimization/tradeoffs of Line-Of-Sight (LOS) vector-pointing focal-plane error driven by higher IV transmissibilities through low-damped structural dynamics that stimulate optical elements. Unique analytical disturbance results for orbital HST accelerations are described applicable to microgravity efforts. Conclusions, lessons learned, historical context/insights, and perspectives on future applications are given; these previously unpublished data and findings represents a valuable resource for fine-pointing spacecraft or space-based platforms using RWAs, Control Moment Gyros (CMGs), Momentum Wheels, or other ball-bearing-based rotational units.
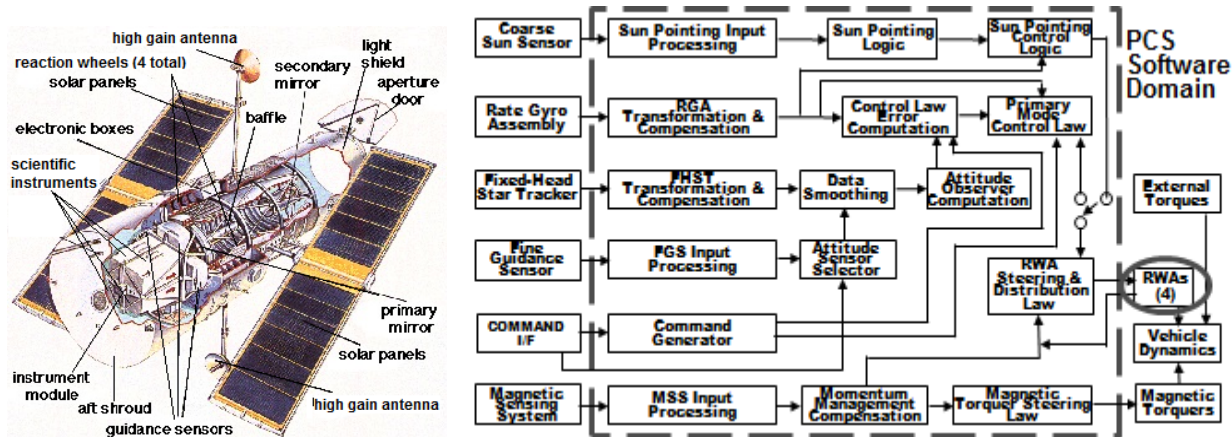
Figure 1. HST Deployed Configuration Cutaway & PCS Block Diagram Highlighting RWAs[1,2]

[*] Lockheed Martin Space Systems Company, Sunnyvale, CA

Introduction/Background: HST Pointing Accuracy using High-Performance/Low IV RWAs

Spacecraft Attitude Control Systems (ACSs) use Inertial Measurement Units, along with other sensor data inputs (Star Tracker, Sun Sensor, Fine Guidance Sensor (FGS), etc.) to Command and Data Handling or Line-Of-Sight Computer control algorithms to command inertia wheel counter-torque outputs in a traditional 3-axis momentum-management scheme (Fig. 1)[1,2]. HST's PCS uses 4 RWAs (i.e., variable-rate, fixed-spin-axis units) in an overall canted-pyramidal arrangement to generate torques for large target-to-target maneuvers/attitude changes (~6°/min) as well as for highest-precision fine-pointing operation.

HST LOS Critical Performance System Jitter Dependence due to RWA Induced Vibrations

HST achieves stringent LOS pointing stability (top-level specified at <7 milli-arcseconds over 24 hours) on celestial objects for long exposures using a structured flow-down budgeting methodology[3]. Analogous means have been refined and applied to other space platforms (e.g., International Space Station microgravity[4]). Imaging can take hundreds of hours via 20-minute exposures; typically 2 per orbit. Repeatable LOS pointing accuracy is <0.01 arcsec (over 100 hours). FGSs detect angular deviations due to on-orbit disturbances (see Table 1 sources[5]) to generate countering minute RWA rotation speed changes to maintain PCA LOS/attitude control; down to <~2 milli-arcseconds as sub-allocated. Other fine-pointing satellites obtain LOS levels via alternate ACS architectures/units (see Table 2[5]). Note that there is a fundamental ACS/PCS tradeoff (in normal attitude hold mode) between smaller RWAs (correspondingly small rotor mass and potentially less stringent residual unbalance) operating at higher maximum rotation rates (much higher IV); or using a larger RWA, that, if driven to tight residual unbalance limits, spins significantly slower (typically much lower IV). It may be more upfront affordable to impose tighter tolerances/balancing in smaller RWA rotor-bearing assemblies, but, as discussed below, may not be overall optimal. RWA IV limits get significant attention due to several inherent aspects: 1) rotation rate can assume any value in a wide spin-rate range, and 2) commanded rates reached and held (i.e., steady-state) dwell sufficiently long for fully-saturated resonance excitation at structural dynamic mode frequencies.

Table 1. Fine-Pointing Satellite Disturbance Examples with Reaction Wheels Highlighted[5]

Source	On-Orbit Satellite Disturbance Type	Mitigation Approaches
Orbital Torques	Atmospheric Drag, Gravity Gradient, Solar Pressure/Impingement, Residual Magnetic Momentum, Thermal-Radiant Field Changes	Orbit Choice, Minimizing Drag Area, Align Center-of-Pressure/Center-of-Mass
Operations	Commanded Maneuvers/Slews Stimulating Low-Damped Structures	Profiling, Ops Constraints/Stay-Outs
Mechanical	Gimballed Antennas, Solar Array Drives, Thermal Electric Coolers, Cryocoolers, Maneuver-Induced Excitations, Thermal Creak/Snap	Body-Fixed Antennas/Solar Arrays, Stiff Structures, Isolation, Profiled Maneuvers
Sensor	Star Tracker Errors – Noise Equivalent Angle, Spatial/Centroiding Errors, Star Catalog Errors, Velocity Aberration, Alignment Variations/Errors Gyro Errors - White Noise, Random Walk, Bias, Scale Factor, Alignment	Higher Quality/Performing Sensors, Better Filters/Estimators
Actuator	*Reaction Wheels* Command Noise, Command Quantization, Residual Static Imbalance, Dynamic Imbalance, Bearing/Drive Harmonics	Higher Quality/Perf. Wheels, Higher Control Bandwidth, Isolation Approaches

RWA Concept-of-Operations (CONOPS) and Basic Induced-Vibration Test Data Considerations

Most HST disturbers (Fig. 3), if threatening jitter limits, can typically adjust their operations, i.e., selectively power off, switch operating modes/profiles, modify duty cycles, and/or transition to alternate capabilities. However, using RWAs creates a unique situation due to operating constantly to maintain HST stability[6]. Also, since constantly commanded torques react to small always-changing external torque effects/phenomenon, RWA rotational rates do not have a priori predictability during each orbit's phases. As a result, there arose a focused demand for IV analytical investigations along with other disturbance source

characterizations; subsequently prompting additional analytical studies to minimize HST LOS jitter impacts as described herein.

PCS analyses originally showed RWA orbital rotation rate predictions of up to 5 Hz (4 RWAs operating); with a potential reach to 10 Hz (600 RPM) under rare unfavorable pointing attitudes. However, estimates later climbed to ~20 Hz (1200 RPM) considering the additive effects of: 1) higher-than-normal solar-cycle activity (where Earth's ionosphere expands causing higher atmospheric drag torque), 2) lowest-possible orbit altitude forecasts (from later-than-expected Space Shuttle service mission/boosts originally planned to occur ~5 years), and 3) assuring mission capabilities in the unlikely event of an RWA or magnetic torquer failure. Note that, due to RWA criticality, HST studies have been undertaken to find approaches to maintain stability if up to 2 RWAs fail[7]. Above worst-case rates and margins set upper bounds for LOS jitter studies.

Table 2. Spacecraft LOS Error Control Methods, Pointing Accuracies/Stabilities, & Examples[5]

| Spacecraft Pointing Accuracy Approximations Obtained via Various System Approaches/Architecture Implementations		Spacecraft Relative Approximate Pointing Accuracy Requirement Level
Pointing/Stability Performance Sensors (each step down includes data/improvement from above)	Pointing Accuracy (arcsec, 3σ)	
Two Star Trackers	60-100	
Adding Gyros	30-60	Typical Commercial Stabilized Satellite
Co-locate attitude sensors with instrument	3-30	Geoeye2 & SIM
Improving Star Catalog	1-3	Widefield Infrared Survey Explorer (WISE)
Using Instrument to Sense Orientation or Using Fine Guidance Sensors	0.1-1.0	Reference Spacecraft & A2100 Variants SIRTF & Deep Impact Spacecraft Flyby Kepler
Fast-Steering Mirrors/Advanced Isolation Systems	0.003-0.1	Extrasolar Planetary Imaging Coronagraph (EPIC)
Systematic Managing/Reduction of all Pointing Error Sources + Interferometric Star Sensor in Optical Path + Source-Structural Mode Separation/Decoupling	Sub-milli-arcsec	Hubble Space Telescope
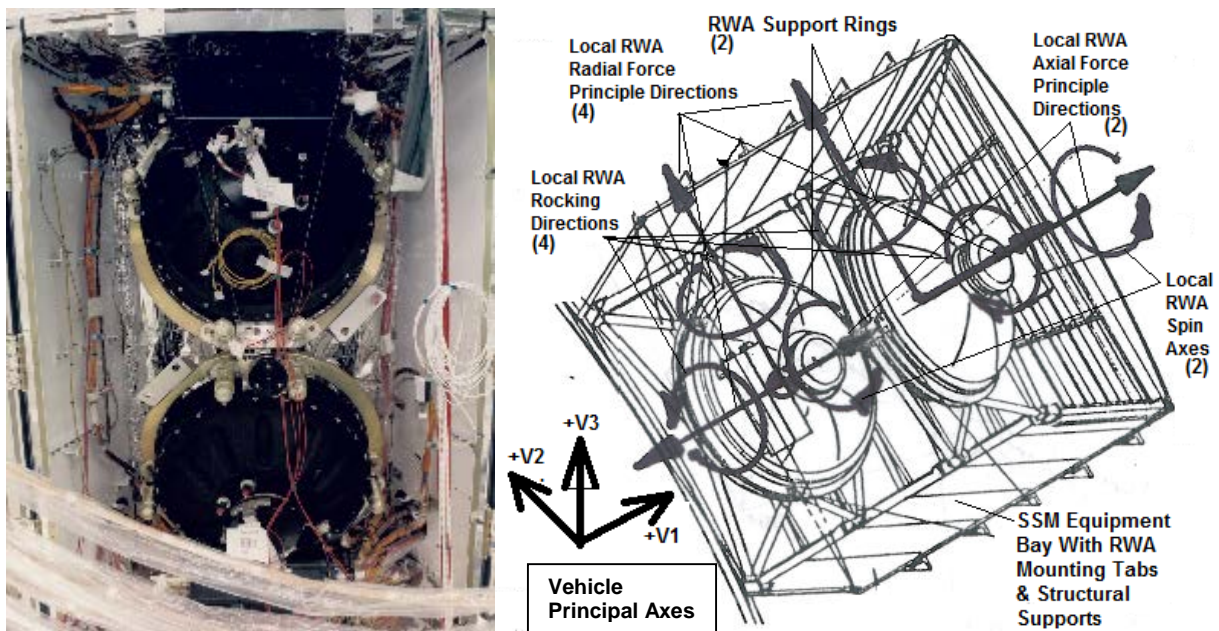
Figure 2. RWAs (2 of 4) in HST SSM Locations & Diagram of Local Principal Directions/Orientations
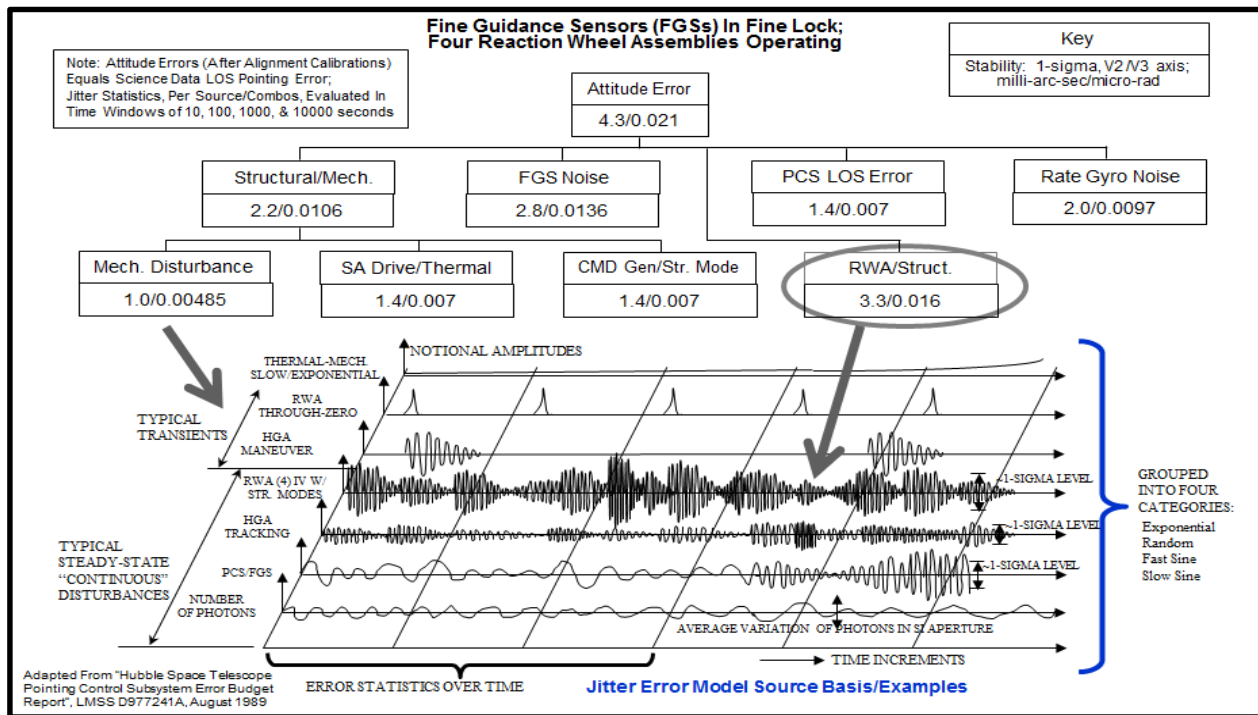
Figure 3. HST SSM PCS Pointing Error Budget & LOS Notional Disturbance-Managed Elements[3,8]

RWA Fundamental Mechanical Noise Vibrational Disturbances Relevant to HST Induced Jitter

RWA IV noise characteristics fundamentally emanate from intrinsic core/assembly imperfections, but can change due to micro-effect combinations; e.g., bearing surface lubricant re-distribution over time can create small non-deterministic detectable deviations. Dynamic fine-balancing is a proven approach to minimize IV; specifically at basic rotation rates (i.e., 1.0 harmonic ratio). IV macro-characterization is not normally of much concern except for predicting end-of-life issues in many rotating assembly applications; but much more critical when applied to highly sensitive transducer/sensor platforms. Although judicious drive motor current monitoring can track long-term bearing friction changes/instabilities, it cannot reliably detect nor correlate well to small IV changes along RWA force/moment axes. Detailed, in-situ, and statistically-valid data are needed to quantitatively ascertain maximum expected IV levels and bound variations/uncertainties; more specifically, design-specific root sources, secondary empirical manifestations, trends/correlation, and externally-imposed conditions that can directly impact jitter limits, system allocations, and margins. The effort documented here was first driven solely to enable HST jitter verification efforts for comparison versus specified top-level limits and sub-level budgets, since acquired IV data are simply input sources for jitter modeling/analysis forcing-functions. However, due to discovery of jitter's hyper-sensitivity to IV, it became clear after gaining significantly more detailed analytical data (discussed below) that contributions from harmonics and ground-to-orbital transitions must also be known/bounded for credible on-orbit predictions. Prior to data compilation, wide speculative ranges (i.e., orders-of-magnitude) existed regarding possible worst-case changes due to relatively modest effects. Alternately, if variability found can challenge IV measured under highly benign lab and handling situations, what unforeseen excessive IV might result from much more severe disturbing effects (e.g., temperature/pressure changes, or launch-ascent vibrations).
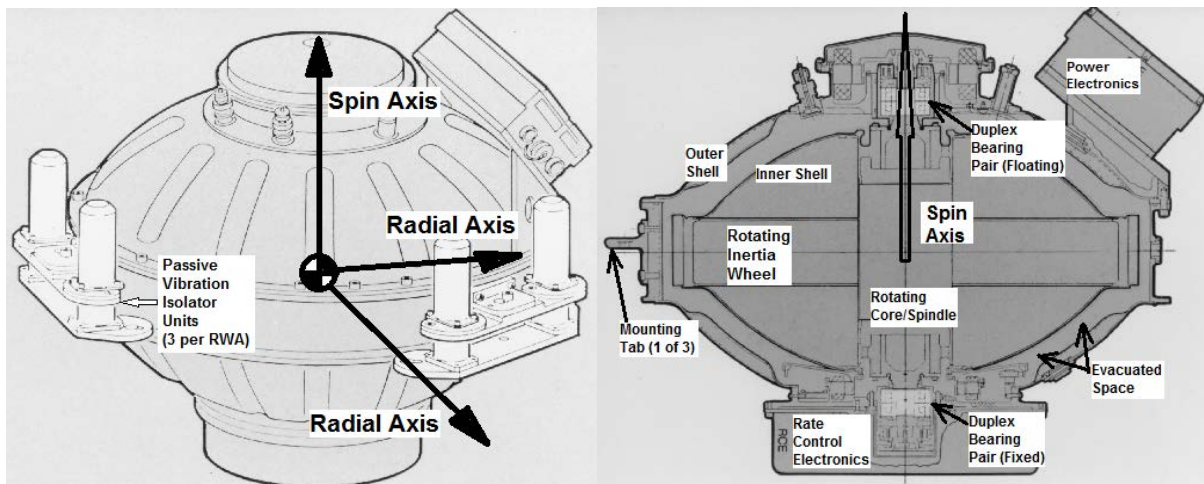
Figure 4. RWA Local Principal IV Directions (Shown on Isolators) & Cutaway Mechanical Features[9]

Fundamental RWA IV Disturbance Characterization: Accompanied by Higher Harmonics

Prior program experience clearly demonstrated that RWA fine-balancing methods – along with significant margins (vs. required limits), performed at minimum-detection levels on high-stiffness test fixtures at rated design speed (e.g., 3000 RPM) with repeated trial-and-error reductions, were successful. At first, because HST RWA imbalance/IV is specified across a range of predicted on-orbit operating speeds, basic 3-axis IV force amplitude data was measured and reported at agreed-to increments of 500 RPM. As RWA IV verification occurred (circa 1984) flight unit acceptance test data were requested. Additionally, to compare value trending versus precursor Engineering Evaluation Unit that supported HST proposal efforts' fundamental performance analyses, spectral plots (force-amplitude-vs-frequency) at selected 200 RPM increments were obtained. It was noted that, while attaining required fine-balance levels with significant margins (i.e., 1.0 radial force harmonic), additional RWA high-amplitude IV peaks (Fig. 5) became prominent (not suppressed by fine-balancing), the first indicator of prominent harmonic content amplitudes that tower over primary IV (~10 times balanced 1.0 harmonic level). At the time, high-frequency harmonics/ratios were seen as an interesting curiosity and not explicitly addressed or enveloped in jitter analytical assessments. PCS experts were not concerned because this IV content was so far beyond practical active control limits.
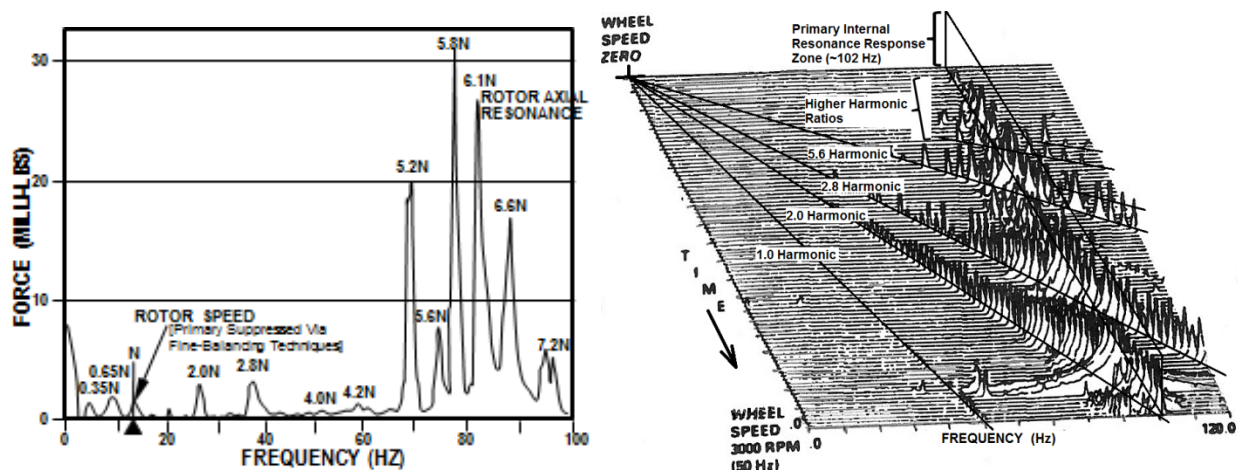

Figure 5. Typical RWA IV (800 RPM/13.33 Hz) & Waterfall-Style (Slowly Increasing Speed) Plots[9]

Early HST RWA-Induced Jitter Tenets/Insights Driven by First Principles and Simplified Analyses

Early HST studies, founded in approaches used on classified satellites, were solely devoted to predicting disturbance effects on an LOS central pointing vector along with minimizing other known image-distorting effects (e.g., tight thermal control, PCS-specific sources) along with large separation of primary structural mode frequencies from the maximum active control bandwidth frequency (target of 5-to-10x). To support this, Lockheed's proposal efforts built a representative full-scale Structural Dynamics Test Vehicle, a medium-fidelity prototype/demonstrator with flight-like structural components' design, analysis, materials, fabrication, and test approaches. It was also sufficiently versatile to support ongoing development efforts. This Structural Dynamics Test Vehicle formed a core structural building block subsequently detailed and outfitted (circa 1987) as the Smithsonian's National Air and Space Museum HST exhibit article[10]. Although RWA IV forces are small (conveniently measured in milli-lb/milli-newtons) inputs to a mammoth 11500-kg (~25000-lb) spacecraft, HSTs milli-arcsecond-level LOS resolution/stability jitter requirements (~100X below prior satellite limits) posed a substantial analytical and testing challenge. RWA's required fine-balance limits (see below) relate directly to primary (1.0 harmonic) IV amplitudes at rotation speed(s). Engineering tasks focused on 4 areas perceived as the most-difficult for achieving stringent jitter levels:

1) High "Scissors Mode" (Fig. 6) frequency, wherein the inner Optical Telescope Assembly and outer Support Systems Module (SSM) structures pseudo-kinematically pivot in opposite directions (pitch & yaw axes), is highly dominant jitter contributor; driven as high as practicable (target >15 Hz).
2) RWA rotor size to be relatively large and kept at low operating speeds (nominally <5 Hz) to minimize primary unbalance radial forces (believed highly dominant) to avoid stimulating Scissors Mode jitter.
3) RWA radial force driven to minimum attainable levels for state-of-the-practice-unbalance/IV-setup detection levels (<milli-newton) by applying challenging unbalance/tolerance minimizing approaches.
4) RWA bearings were specified to be of proven tightest tolerances, acquired in same-production lots, and then checked by fine balancing for *acceptable* primary balance disturbances. In principle, it was thought that higher-frequency vibrations were insignificant (and not specified) compared to the paradigm on runout/unbalance threats: more extended efforts not considered needed nor practicable.
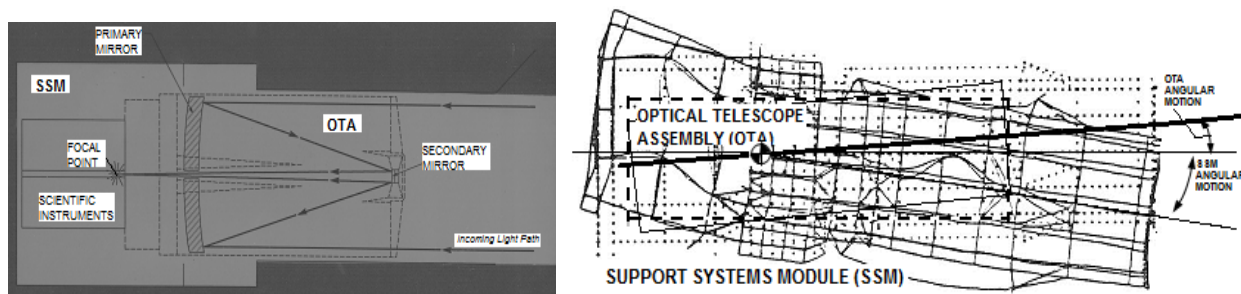

Figure 6. LOS Reflective Optical Path Diagram & Scissors Mode Dynamic FEM Plot (Pitch Direction)[9,11]

Lessons Learned: Historical Background and Perspectives on Unforeseen HST Jitter Problems

Early HST efforts (rudimentary computing technology) predicted structural dynamic disturbances by use of laborious hand calculations and relatively simplistic calculator/computer analysis. Finite Element Model (FEM) static stress analysis was barely more advanced and transitioning simultaneously alongside classic hand calculations/checks; as an example, stress analysis result uncertainties still necessitated classic full-scale extensively-instrumented Proof Load tests. Maturing during HST Preliminary/Critical Design Review efforts (circa 1978) were sufficiently capable, more readily available, and reasonably reliable Structural Dynamic modeling-analyses tools to begin to compute end-to-end disturbance/jitter characteristics with improved details including, for the first time, more refined secondary effects. Around 1982, emergent ray-trace modeling tools (e.g., employing Zerneke polynomials) provided actual magnification-derived LOS values for individual optical elements moving/distorting relative to each other and a centralized reference

LOS path. Dynamic FEMs[11], due to computationally intensive eigenvalue calculations, were judiciously reduced (limited to ~900 dynamic Degrees-of-Freedom (DOFs) and 412 nodes-gridpoints) as compared to much larger DOFs (>10 times) in structures-stress static models. This helped offset conflicting needs of having adequate analysis fidelity yet computer runs (via the most capable computers available) that could complete within practical timeframes. These were typically a cluster of all-night runs (~15 hour run-time if not encountering convergence problems) taking several days to compile 157 modes (0-to-75 Hz). Many cross-checks/iterations occurred on the reduced dynamic FEM to prove stiffness properties replicated more refined stress FEMs plus mechanical assembly prototype test results. High criticality was placed on meeting regular re-analysis deadlines, so a significant amount of pre-computation efforts were expended on sparse-matrix sequencing methods and trial-and-error connectivity-optimization schemes to compress run-times lower within an assortment of additional competing constraints, e.g., most capable computer available (Sperry Univac 1100/92; 36-bit, 133MFLOPS) vying with top-priority classified programs' runs.

During a typical LOS jitter evaluation (re-assessed often due to evolving mass properties data, structural refinements, and updates of stiffness values), that involved checking all mechanical disturbers (e.g., tape recorders, high-gain antenna gimbals, RWAs), an unexpected RWA jitter impact was unexpectedly discovered coming from a very subtle model input coding error. Upon reviewing a typical RWA overnight run's graphical jitter results, a high-amplitude (i.e., ~5 times normal; significantly exceeding specification) spike of jitter appeared at a previously unseen higher frequency (~30 Hz) that had no analog in any prior results. This highly anomalous result prompted an intensive and focused effort of input data review and re-checks/cross-checks. Using some model insights (e.g., what compound dynamic modes were showing high generalized responses near that frequency) and localization (e.g., what input-output response combinations are proximate to responsive LOS optical elements) plus multiple trial-and-error eliminations, appearance (and disappearance) of the large jitter value was related to a single RWA mass property input line of code. Although continuation of data values on a line was allowed by the modeling-analysis program (with no error indications), data extensions were truncated/ignored at 80 characters due to prior program limits of punched card inputs not noted in computer code documents. Subsequently, this got corrected to allow *unlimited* input strings via continuation symbols. However, this investigation created a totally new serendipitous insight beyond just a trivial code error. This tiny error caused a specific RWA mass property (local "rocking" rotor inertia) to be reduced, but valid within the code's execution/error detection abilities. Thereby, on the given base stiffness (a validated value), driving RWA local IV disturbance moments to more effectively stimulate a very-high-frequency complex mode (~90 Hz) previously not believed to be a jitter issue. Amplified by the local RWA mode, IV inputs were injecting much larger generalized modal moments directly into the rigid SSM core/base structure; in turn, efficiently driving a previously unrelated angular coupled modal displacement at a higher and complex-system-mode frequency involving a smaller relay Optical Telescope Assembly optical element, namely secondary mirror motion. This created the very first analytical awareness that, after significant mitigation of the 4 main RWA-scissors-mode/fine-balancing concerns discussed above, a "new" system issue suddenly developed into a formidable jitter threat from RWA high-frequency inputs (not amenable to simple unbalance corrections) stimulating local IV-input modes that could then couple with higher frequency resonant modes locally dithering optical components. Such high-frequency modal response, combining with test-derived low structural damping (~0.005) at small forcing amplitudes, needed much less (~25 times) input forces/moments than previous IV/unbalance disturbance values. HST's secondary mirror's suspended mass is ~5% of the primary mirror's mass; minute angular movements through a very high effective optical magnification displaced it sufficiently to impact LOS jitter.

This near-overnight revelation radically transformed previous jitter-problem paradigms. Engineering pursuits immediately shifted to ferret out high-frequency disturber characteristics, along with much more attention to accurately model refinements of input disturbers' mounts and regions near optics, especially proximate support structure stiffness elements. All this while still adhering to severely limited FEM DOF detailing/frequency-range constraints. This also led directly to assuring highly optimized (i.e., high local stiffness still within tight mass limitations/budgets) RWA support-mount structural element representations to drive local response modes up in frequency (target >60 Hz, based on the next higher local compliance being RWA mounting-tab-to-outer ring stiffness that was difficult to redesign), without creating new side

effects, e.g., more optical-mode complex cross-couplings. A highly-iterative effort, involving stress, design, and manufacturing engineers, eventually found a viable design approach meeting strict mass limits.

As a related aspect, significantly stiffer base/mount (in local DOFs) and improved knowledge of RWA high-frequency outputs initiated a quick-response RWA vibration isolation feasibility assessment. Those results led directly to developing a unique fluid-damped passive vibration isolation system (e.g., Fig. 4), applying a pseudo-kinematic interface approach while retaining HST Orbital Replaceable Unit capabilities via astronauts using standard tools[8,9]. Findings and techniques were later applied to large aeronautical and aerospace systems[12,13]. Insights also directly caused investigation of IV high-frequency harmonics, how IV is modeled/bounded, sources for IV variation amount evidence, and data regarding IV measurements of ground-vs-orbit uncertainties/variations[14]. Concerns also emerged about the potential for a dense field of IV harmonics (see Fig. 5 rightmost resonance zone) to converge via a non-obvious combination of input forces-moments to create a "perfect resonance storm", collectively stimulating a reactive high-frequency complex mode involving several smaller optical components. Data on realistic damping values were also investigated due to emerging evidence that classic high-amplitude damping approaches (i.e., elastomerics) tend to substantially diminish at low force levels; prior analyses used damping derived from high-amplitude forces (~3%; i.e., launch-level vibrations). Fortunately, due to efforts attacking 4 jitter priorities (above), IV test setup detection capabilities could effectively collect sufficiently sensitive amplitude-spectral data with minimal modifications thereby avoiding yet another added development-improvement effort. The author had sole responsibility for dynamic modeling, model validity, substantiating damping data, RWA isolation system requirement development, and jitter result accuracy verification during this time. Regularly, separate high-detail dynamic models were rapidly created for a key subassembly or unit to then integrate a simplified version into the full HST model that closely replicated local mode frequencies/shapes. Efforts included successful conduct of a thorough model audit/review with NASA Subject Matter Experts. Due to such attention/refinements, subsequent HST modal tests concluded that analysis results compared very well with the pre-test structural dynamic model[2]. For a period, circa 1985, this Level 1 RWA-IV-based LOS jitter requirement threat was the foremost program technical concern, receiving considerable attention and visibility at quarterly reviews. Although not a heroic save of HST performance, its importance is notable.

RWA IV Disturbance Source Considerations Relative to Classic Wheel Bearing Imperfections

HST RWAs are deemed state-of-the-art (for their size) due to several unique aspects: 1) strict screening of matched duplex bearing sets via preliminary runout measurements and added data checks acquired in pre-acceptance runs on a fine-balanced EDU rotor (e.g., <50% yield for flight-qualified ABEC 9 production lots), 2) unusually high number of fine-balance iterations, 3) attention to spectral signature/trends in fine-balance iterations, and 4) lubricant (derived Andok C) tailoring for robust stability in HST operating conditions. The RWA vendor was highly motivated by a potential to advance existing knowledge of low-noise wheels. IV arises from 3 primary imperfect root causes: 1) rotor-bearing assembly mass unbalance/asymmetries, 2) minute bearing/race/retainer imperfections, and/or 3) drive configuration/physical forces. These can be separately differentiated, but, as combined, create the total disturbance output spectral signal. In theory, using first-principle fundamental physics, precise definition of bearing parameters/geometry, tolerance build-up, and misalignments would allow near-perfect knowledge of all detected IV ratios and provide some indication of relative intensities. However, in practice, spurious microscopic-level effects (e.g., lubricant/tribological interactions, surface conditions/finish, temperatures, minute ball bearing preload fluctuations, etc.) manifest as deviations in internal contact-surface placements and amplitude excursions which exponentially grow with rotation speed, but are not possible to consistently predict or practicably ascertain in use. If a candidate geometric-based imperfection(s) is below a readily measurable threshold (or is excessively difficult/costly to investigate or measure further), a deeper quantitative root is not tractable; e.g., ball bearing/cage localized out-of-roundness or duplex-pair-to-duplex-pair eccentricities.

Primary Static-Dynamic Unbalance on Rigidly Mounted Rotating Masses as Applied to RWAs

Rotor balance and related bearing stability/dynamics is well studied and analyzed[15,16] and summarized here for high-precision RWAs. Figure 7 shows key parameters and balance quality grades. Once specifying a

grade/limit, a maximum allowable residual unbalance (e.g., in g-mm/kg) is determined for the rotor mass and prescribed service/reference speed. Note that maximum allowable residual unbalance calculations assume that rotor mass is evenly distributed about the center-of-gravity and along the shaft between bearings. For reference, a typical (~10 lb$_{(mass)}$ rotor) spacecraft RWA static balance limit is 0.007 oz$_{(mass)}$-in; equating to 44 μ-inch (1.1 μ-m) unbalance offset. HST's large RWA (44 lb$_{(mass)}$ rotor) spec limit is 13.4 μ-inch (0.34 μ-m). One RWA's post-environment IV test resulted in 2.5 μ-inch (0.063 μ-m), an 80% margin.
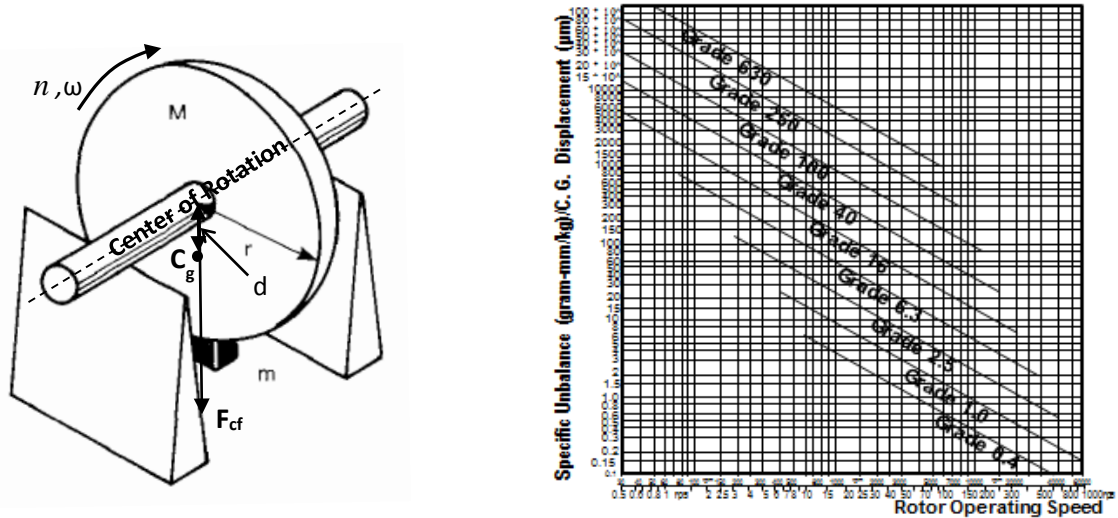

Figure 7. Rotating Mass Unbalance Parameters & ISO Standard 1940 Balance Quality Grades[15]

Output sinusoidal centrifugal force amplitude (F$_{cf}$) is related to rotor unbalance parameters by the following:

$$F_{cf} = M*d*\omega^2 = M*d*(2\pi f)^2 = M*d*\left(2\pi\frac{n}{60}\right)^2$$

Where M is rotor mass, d is effective distance between rotor center-of-rotation and center-of-gravity/mass, (C$_g$), and operating rotation rate is given by n (RPM), f (Hz), or ω (angular velocity in radians/second). For a designated ISO Standard 1940 Balance Quality Grade, the fundamental relationships are:

$$e = \frac{\upsilon}{1000*\omega} = \frac{\upsilon}{1000*2\pi f} = \frac{\upsilon}{1000*2\pi*\frac{n}{60}}$$

Where e is specific residual unbalance (gm-mm/kg)/displacement (μm), υ is balance grade (based on angular rate and relatable to effective radius d via rotor mass); rate parameters are as above. Resulting RWA unbalance (1.0-ratio) IV propagates at a frequency matching the commanded rotation frequency.

IV-Related Empirical Findings Relative to Bearing Geometries and Geometric Imperfections

Since IV characterization stems from fundamental bearing design aspects, geometric parameters lead to IV ratios/relationships. For example, HST RWA bearings (a tailored variant of commercially available 304H-type angular contact ball bearings) have design dimensions shown in Table 3 relative to Figure 8.
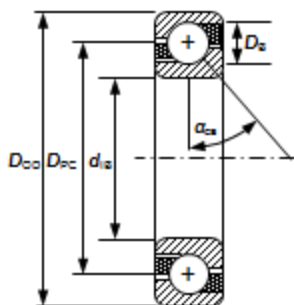
BEARING PARAMETER	304H NOM. VALUES	101-TYPE NOM. VALUES
Inner Bore (d$_{IB}$)	20mm (0.7874 inch)	12mm (0.4723 inch)
Outer Diameter (D$_{OD}$)	52mm (2.0472 inch)	28mm (1.024 inch)
Pitch Circle Diam. (D$_{PC}$)	35.6mm (1.402 inch)	20.2mm (0.796 inch)
Ball Diameter (D$_B$)	11.1mm (0.438 inch)	4.7mm (0.1875 inch)
Number of Balls (N)	8	10
Contact Angle (α$_{CA}$)	18.6 degrees	15.0 degrees
Material	52100 CEVM	52100 CEVM
Tolerance Class	ABEC 9	ABEC 9
Max. Runout Allowed	.0012 mm (.000047")	.0012 mm (.000047")
Bearing Configuration	2 DF Duplex Pairs	2 DF Duplex Pairs

Figure 8 and Table 3. 304H & Comparable 101H-Series Bearing Basic Design Parameter Values [9]

Bearing Retainer Vibration Harmonic Ratio Calculations for a Forced Rotation Situation

Based on classic bearing theory, with an analog to planetary gear systems with a static outer ring gear and driving-torqueing sun gear, the two fundamental relationships between vibrations caused by inner/outer ring raceway ball-contact imperfections are related via the cage/raceway rotational speed. The ratio of bearing cage-retainer speed/frequency to inner rotor shaft speed/frequency is given by the equation:

$$\frac{f_c}{f_r} = \frac{1}{2}\left(1 - \frac{D_b}{D_{pc}} * \cos\alpha_{CA}\right)$$

Where f_c is cage/retainer rotation speed/frequency, f_r is inner ring/shaft rotation speed/frequency, D_b is nominal ball diameter, D_{pc} is the pitch circle diameter, and α_{CA} is the nominal contact angle. This leads to a key ratio value (for 304H) of 0.35. Similarly, the ratio relative to outer ring speed/frequency is given by:

$$\frac{F_c}{F_r} = \frac{1}{2}\left(1 + \frac{D_b}{D_{pc}} * \cos\alpha_0\right)$$

Where F_c is cage/retainer rotation speed/frequency, F_r is effective outer ring passage speed/frequency, and other parameters are the same as above. This leads to a second key ratio value (for 304H) of ~0.65.

Non-spin-axis ratios for a 304H duplex bearing pair would all have a theoretical basis origin due to one of the following ratios: 0.35, 0.65, 1.0, 8.0 (same-ball inner return ratio), or 0.0588 (1/17; same-ball-retainer geometric alignment return ratio). Other ratios are known to exist (i.e., Fig. 5), however, were of significantly lower intensity or are difficult to identify at RWA dwell speeds prescribed in test procedures. For HST RWAs, IV tested/tracked/reported ratios (set of 8 neglecting 0.65 detection issue) are in Table 9.

Table 9. HST RWA Bearing Set Basic IV Tested/Tracked/Reported Harmonic Ratios

Theory-Based Ratio	Empirically-Established Ratio	Description of Root Source/Cause	Sig. Figures Known
0.3521	0.35	RATIO OF BEARING CAGE/RETAINER SPEED TO ROTOR SPEED	2
0.6479	Detection Difficult	RATIO OF BEARING CAGE/RETAINER SPEED TO OUTER RING PASSAGE	2
1.0000	1.00	MISALIGNMENT OF ROTOR CENTER-OF-MASS & SHAFT ROTATION POINT	AS PRECISE AS RWA
2.0000	2.00	SECOND HARMONIC OF 1.0 (RACE-TO-RACE MISALIGNMENT/WHIRL)	AS PRECISE AS RWA
2.8168	2.82		3
5.1832	5.18	N (# OF BALLS - 8) TIMES 0.65 (BALL PASSAGE ON INNER RACE)	3
5.6336	5.60	SECOND HARMONIC OF 2.8 (BALL PASSAGE ON OUTER RACE)	3
--	7.50	CAUSE NOT KNOWN WITH CERTAINTY; ONLY EMPIRICALLY DERIVED	~2
--	8.50	CAUSE NOT KNOWN WITH CERTAINTY; ONLY EMPIRICALLY DERIVED	~2

At first RWA IV data assessments, there was no analytical-empirical basis correlating a harmonic's amplitude to another harmonic's amplitude thus all harmonics (and their amplitude variations) were perceived as individual and independent uncorrelated entities. See discussion below concerning the validity of this viewpoint. For 101-type bearing RWA assemblies, key ratios are somewhat different, as delineated in Table 10.

Prompted by pure-analysis deficiencies, empirical IV data have dominated quantifying RWA disturbance macro characteristics, harmonic ratios, IV levels, variations, and relative trends. Extractions from refined IV data studies led to a need for a comprehensive common basis to compare resultant IV macro-effects. Per classic intrinsic physical principles, some element of bearing Geometric Runout (expressed via a geometry-related value that generally rises and falls in league with overall IV amplitudes) is presumed fundamentally responsible for non-spin-axis harmonic vibrations. Since dominant effects (e.g., primary unbalance) are

directly relatable to classic parameters of imbalance coupled with bearing "goodness" (similar to long-standing static/dynamic rotating assembly methods), and since larger unbalance (very generally) causes a 2nd-order growth of all noise components as rotation rate builds, an alternate means of absolute/relative "geometric" error was sought. Setting aside design-specific harmonic ratios, an equation form is desired that can be reverted to classic unbalance-runout types of values/assessments. Also, unlike primary unbalance, its value is to enable directly relating bearings independent of rotor mass. A summary treatise, reference perspective, derived relationship, and example values for this methodology/criteria follows below.

Table 10. 101-Type Bearing Set Basic IV Tested/Tracked/Reported Harmonic Ratios

Theory-Based Ratio	Empirically-Established Ratio	Description of Root Source/Cause	Sig. Figures Known
0.3862	0.385	RATIO OF BEARING CAGE/RETAINER SPEED TO ROTOR SPEED	2
0.6138	Detection	RATIO OF BEARING CAGE/RETAINER SPEED TO OUTER RING PASSAGE	2
1.0000	1.00	MISALIGNMENT OF ROTOR CENTER-OF-MASS & SHAFT ROTATION POINT	AS PRECISE AS RWA
2.0000	2.00	SECOND HARMONIC OF 1.0 (RACE-TO-RACE MISALIGNMENT/WHIRL)	AS PRECISE AS RWA
3.8623	3.88	10 (# OF BALLS) TIMES 0.39 (BALL PASSAGE ON OUTER RACE)	3
4.0000	4.00	THIRD HARMONIC OF 1.0 (RACE MISALIGNMENTS/COMPOUND WHIRL)	AS PRECISE AS RWA
6.1376	6.14	10 (# OF BALLS) TIMES 0.61 (BALL PASSAGE ON INNER RACE)	3
--	7.17	CAUSE NOT KNOWN WITH CERTAINTY; ONLY EMPIRICALLY DERIVED	~2
7.7246	7.72	SECOND HARMONIC OF 3.85 (BALL PASSAGE ON OUTER RACE)	3
8.0000	8.00	FOURTH HARMONIC OF 1.0 (RACE MISALIGNMENTS/COMPOUND WHIRL)	AS PRECISE AS RWA

Geometric-Based-Error Method Allowing Direct Comparison of Harmonic Disturbance Magnitudes

Based on empirical HST RWA IV datasets plus a quest for comparing similar configuration bearings with other sizes (i.e., varied harmonic ratios) and local directions, a quantity termed "Equivalent Geometry Error" (E_{GE}) was established as a straightforward approach for analytical evaluation based on a least-squares best-fit-curve methodology imposed on IV second-order equations, facilitating direct comparisons related to amplitudes present in compound harmonic IV signals' data. It was intended to apply to any RWA data acquired by similar test criteria and number of data points (i.e., via computing curve-fit second-order coefficients). Fundamental E_{GE} is computed for a chosen harmonic ratio via the following formula:

$$E_{GE\,n} = C_n \frac{\Sigma\,(F_{ni} * \omega_{ni}{}^\wedge 2)}{\Sigma\,(\omega_{ni}{}^\wedge 4)}$$

Where C_n is a varying constant for a particular harmonic (n) and, for HST RWAs, is equal to the following 4 key values when wheel speed (ω_{ni}) is expressed in revolutions-per-minute (RPM), output sinusoidal force peak amplitude (F_{ni}) is expressed in pounds (lb), and E_{GE} ($E_{GE\,n}$) is expressed in inches (in).

$$C_{1.0} = 821.5 \; ; \; C_{2.0} = 205.3 \; ; \; C_{2.8} = 103.3 \; ; \; and \; C_{5.2} = 30.6$$

When derived in stated parameter units, resulting units are in/lb-min^2. Note these are also relatable independent of DOF. As derived from IV datasets, the number of points used needs to be enough for reasonably consistent computation stability (varies by frequency range), yet not so many to interpose distorting effects of RWA/fixture resonances; points typically range 4-20. This may require insightful judgment/iterations for the optimum number of points for calculations while rejecting data outliers.

Induced Vibration Harmonic Ratios Basis in RWA Spin-Axis Torque/Moment Primary Direction

Spin-axis harmonic ratios are governed by an entirely separate set of physical effects compared to other IV DOFs. Design-specific drive motor physics/construction creates minute fluctuations (termed torque

ripple) in otherwise steady torques imparted to the RWA ring-tab-base-mount rigid structural interface at ratios differing from non-spin-axis forces/moments. HST's RWA motor is a 2-phase, 8-pole, brushless direct-current design with resolver, a configuration resulting in torque ripple harmonic ratios summarized in Table 11. Internal control/filtering features are utilized to minimize all except the 16.0 and 32.0 harmonics. RWA torque ripple limits are standardly specified (with margins), and precisely measured in acceptance tests. Note that, as verified for HST, torque ripple IV dynamics are a negligible (i.e., nearly undetectable analytically or in system tests) contributor to overall optical system LOS jitter for all but the very lowest frequency modes and under assumed worst-case maximum levels. The low torque ripple DOF result is due to convergence of several favorable jitter factors: 1) electro-magnetic origins lead to readily-applied circuit/processing minimization techniques, 2) IV amplitudes are extremely low compared to other local moment DOFs in primary RWA operational speed ranges, 3) high relative rotor inertia, 4) much higher relative rotor structure effective stiffness (i.e., much higher internal rotor torsional mode frequencies), 5) much higher HST structural ring effective stiffness, and 6) intrinsic HST structural dynamic mode impediments to enable stimulating complex-compound optical paths/components to cause LOS jitter. Also favorable is that torque ripple levels are reliably less than required limits, highly stable over time (i.e., no significant wear source), and not measurably affected by operating conditions or environmental changes.

Table 11. HST RWA Spin-Axis Motor-Design-Driven Harmonic Ratios

Theory-Based Ratio	Empirically-Established Ratio	Description of Root Source/Cause	Sig. Figures Known
4.0000	4.00	COMBINED RESOLVER & ELECTRONIC DEMODULATION OFFSET WITH OTHER EFFECTS; DC BIAS OF EITHER SINE OR COSINE WINDING	AS PRECISE AS RWA
8.0000	8.00	ELECTRONIC GAIN MISMATCH; MISMATCH OF SINE/COSINE WINDING CURRENT AMPLITUDE FOR GIVEN COMMAND	AS PRECISE AS RWA
12.0000	12.00	ELECTRONIC NONLINEARITIES	AS PRECISE AS RWA
16.0000	16.00	MOTOR-RESOLVER RIPPLE; RELATED TO WINDING TYPE/CONSTRUCTION	AS PRECISE AS RWA
32.0000	32.00	MOTOR-RESOLVER RIPPLE; RELATED TO WINDING TYPE/CONSTRUCTION	AS PRECISE AS RWA
48.0000	48.00	COMBINED ROTOR-RESOLVER RIPPLE & MOTOR COGGING, DUE PRIMARILY TO MAGNET ATTRACTION NEAR LAMINATION SLOTS	AS PRECISE AS RWA
96.0000	96.00	MOTOR-RESOLVER RIPPLE; RELATED TO WINDING TYPE/CONSTRUCTION	AS PRECISE AS RWA

Feasibility Investigations Validating a Chosen 4-Harmonic Subset for Adequate LOS Jitter Assessment

Upon thorough study of this abundance of potential jitter error contributors and harmonic ratios, there quickly arose a huge obstacle: managing such a tremendous amount of data inputs and output assessment summaries. It seemed a potentially impossible task due to so many separate data/combinational elements:
- Virtually unlimited number of individual RWA IV frequencies to dwell at within predicted range limits
- 157 dynamic modes (to 75Hz) in jitter evaluations; at practical model/analysis computational limits
- 3 LOS jitter axes; vertical, lateral, spin about image plane centerline (HST pitch, yaw, roll)
- 5 RWAs (one spare – but any 4 could be potentially used); each with its own unique IV signature
- 20 possible RWA-location permutations 5 flight-certified RWAs could be in any of 4 flight positions
- 6 local DOF IV input force/moment signals for each RWA; with further breakdown as follows
    20 detectable axial-force harmonic ratios applicable to 1 principal local DOF on each RWA
    28 detectable radial-force harmonic ratios applicable to 2 principal local DOFs on each RWA

- 7 known axial-moment harmonic ratios applicable to 1 principal local DOF on each RWA
- 8 (at least) known radial-moment harmonic ratios applicable to 2 principal local DOF per RWA
- 20 viable flight-unit sets of IV datasets; a mix of partial (i.e., due to penalty re-tests) and full
- 30 axial-DOF isolation system stiffness-damping combinations to evaluate; with and without isolators
- 34 radial-DOF isolation system stiffness-damping combinations to evaluate; with and without isolators

Changing any single one of these elements/parameters results in a different jitter pass-fail value compared to specified limits. Based on prior results, none of these individual aspects could be readily dismissed as insignificant in ferreting out a previously undiscovered but potentially crucial LOS impacting combination. For one specific example, most results (but not all) showed jitter-budget peaks/threats (within operational frequencies) dominated by axial forces, where fine-balancing has no mitigating effect; a counterintuitive outcome compared to conventional wisdom that radial force unbalance is most likely to threaten jitter. The potential permutations seemed endless, most formidable being so many harmonics present in the 5 RWA DOFs. One fortunate aspect was, due to such low damping (i.e., 0.005), the computed damped frequency of a potential high-jitter-response mode is essentially equal to its computed undamped frequency (within ~2-3%), therefore, jitter analyses were constructed to evaluate response at each specific computed mode frequency (i.e., eigenvalues; 157 for full HST orbital model), with inserts of intermediate-increment values smoothly bridging the region between a computed mode peak and the overtaking rising portion of the next-higher-frequency jitter spike (again, due to low damping's very sharp peak). Once these means were accomplished (in conjunction with a separate jitter assessment determining solid baselines for 4 most-likely flight RWAs with adequate data choosing a representative and full dataset for each), studies shifted to compare jitter results using a robust subset containing the 4 most prominent IV harmonic ratios (i.e., 1.0, 2.0, 2.8, and 5.6 in 2 radial and 1 axial DOFs) versus an entire set of detected harmonic ratios (30 axial; 34 radial). By comparatively using all harmonic ratios from a representative high-amplitude dataset for each RWA DOF, results showed conclusively that 4 key harmonic ratios (e.g., Fig. 9) are excellent indicators for RWA jitter predictions and establishing a jitter baseline for further isolation and placement optimization studies; while maintaining timely and efficient computational processing and reporting[14].
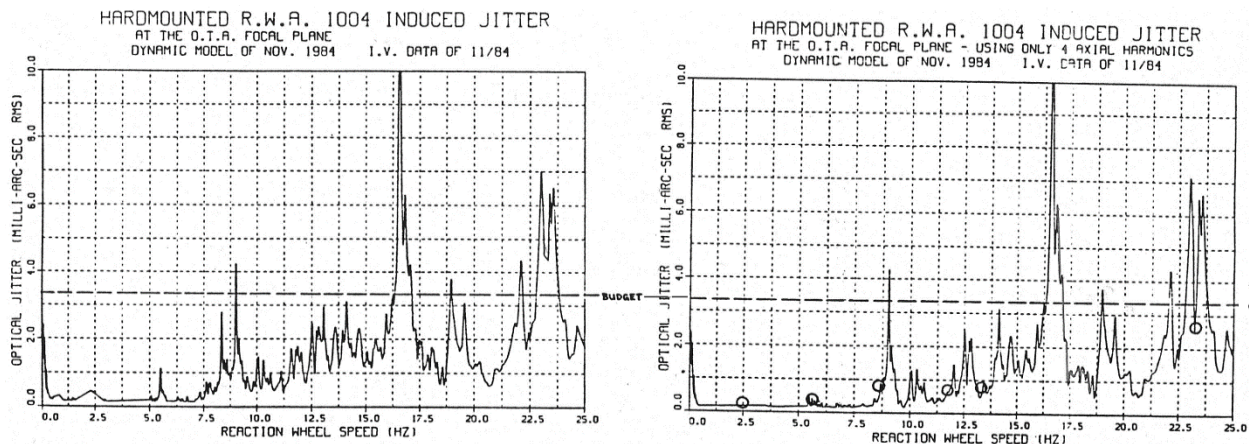
Figure 9. LOS Jitter Results using All RWA IV Harmonic Ratios versus Subset of 4 Key Ratios[14]
[Circles are limited spots where 4 key ratios under-predict jitter spikes compared to full-set results]

Lessons Learned: Newly-Refined Correlative Analytical Investigation for RWA IV Key Harmonics

Fundamental conjecture, based on first principles, initially supposed that residual unbalance coupled with stringent bearing/retainer tolerances define the means to successfully ensure low-IV rotating assemblies. As this IV investigation demonstrated via statistically robust harmonic ratio data mining, there is much more to this basic characterization for a specialized fine-pointing application. Knowing what IV output frequencies,

as a function of realistic RWA operating speeds, are dominant can demand extensive test data and analytical exercises. However, if some ratios are found to be closely correlated, there is the potential to extrapolate or bound overall IV with substantially reduced testing/post-test analysis (i.e., early analyses results can support that a limited test data set affirms upper-level jitter requirement compliance thereby reducing test data collection). It is highly desirable that clear, robust trends emerge readily from straightforward examinations of the IV data collection; e.g., testing a hypothesis that radial force primary unbalance (1.0 harmonic) consistently tracks and predicts axial force 1.0 harmonic (or other ratios) IV data. This data set provides, for the first time, a viable opportunity to quantify potential correlations once any particular rotor-bearing physical properties / harmonic relationships are known within consistent bounds. This creates a practicable set (12) of candidate correlations (relying upon the 4 key harmonic ratios) within each DOF (3; axial force, radial force, radial moment) and dual ratios (4; 1.0-to-2.0, 1.0-to-2.8, 1.0-to-5.2, and 2.8-to-5.2). Extending further, 12 DOF cross-axis pairings are correlated (12; same-ratio pairs). If no strong correlations exist within these 24 IV pairings (some are, in first-order theory, tied to the same root imperfection; while some are not), then reaching for even more obscure relationships would not likely be fruitful for the efforts expended (e.g., test data collection system noise dominates relationships). Until such analysis is conducted, there is no solid analytical basis for common relationships in data sets or root imperfections. The E_{GE} methodology discussed above (via 2nd-order coefficients) serves as a common basis for cross-harmonic comparisons. IV harmonics with relatively poor and good correlations are in Figure 10: E_{GE}s in units shown above. Summarizing, results are mixed yielding some but few strong correlations.
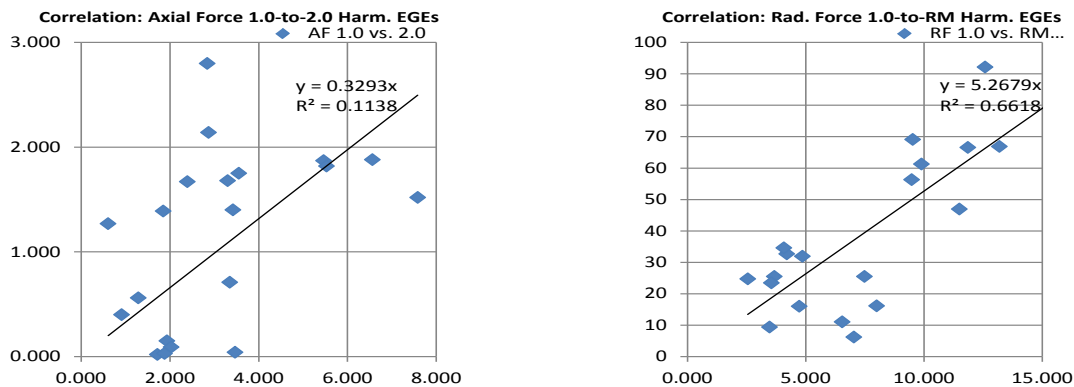
Figure 10: Examples of Relatively Low (AF1.0-AF2.0) & High (RF1.0-RM1.0) IV Data Correlations

RWA IV Analytical Assessment Investigation Overview/Summary

Multiple flight IV datasets, addressing known/available RWA vibrational and variability data sources, are researched, analyzed, and compiled herein; a valuable reference for comprehensive RWA jitter analysis characterizations. Specifically, this treatise: 1) collects, compares, and statistically evaluates 4 dominant harmonics for 20 IV ground-based data sets in local principal RWA axes, 2) exposes rationale for the relative dominance of those 4 harmonics for jitter predictions, and 3) presents comparative data on 32 previously undetected/unknown less prominent harmonics. Values are presented via a combination of summary tables and graphs. This also provides fundamental insights for pre-determining rotor-bearing factors driving IV harmonic ratios, estimating same-size/design bearing characteristics, and solidifying the validity, applicability, and robustness of IV measurements when several factors are considered that may significantly skew actual LOS on-orbit jitter amounts away from test-based analytically-predicted values.

Specific Basis, Background, and Objectives for Overall RWA IV Dataset Investigation Effort

Effects potentially impacting IV values (and are present in ground-to-orbit transitions) have been explored with the RWA supplier's SMEs and summarized below. Specific IV study super-objectives are:
1) determine values and ferret out attributable root causes of IV known variations that directly affect ground-ambient measured IV test data value differences, and

2) determine magnitude bounds for expected variability present in applying IV test data values acquired in ground test lab-ambient conditions to the on-orbit jitter performance analyses.

The two foremost bodies of data/knowledge available to address these study goals are, chronologically:
1) large body of test data accumulated on a comparably-sized CMG production program at the RWA supplier under independent engineering and Research & Development investigations, and
2) 20 IV data sets obtained on delivered RWA flight complement set (4 flight units, 1 spare).

This study combines applicable data available from these 2 key database sources. It also introduces heretofore unpublished additional relevant data and insights gained from:

1) early developmental tests performed on the Engineering Development Model RWA (primarily investigating the effect of different temperature extremes on RWA performance),

2) IV tests performed in support of RWA isolation system program development (primarily concerning newfound evidence that there seems to be more potentially significant RWA harmonics than previously investigated), and

3) numerous discussions conducted between LM and the supplier's technical personnel conducted over a two-year timespan (i.e., primarily concerning the predicted temperature variation effects which are perhaps the most difficult to quantify/bound).

Induced-Vibration Variation Based on RWA Acceptance Test Series Data

Acceptance tests on four flight RWA units (designated 1001, 1002, 1004, and 1005) and one flight spare unit (1003) were completed by the supplier and resulting data packages were delivered to LMSSC and reviewed for completeness and correctness (Ref. 1 & 2). Portions of the full acceptance test results (IV test results) have been extracted and compiled. An investigation was initiated to study and analyze in detail the 20 full or partial applicable datasets (out of 24 total) produced during all flight unit acceptance testing; four early, partially unsuccessful IV tests on the first-produced unit (1001) used a different rotor-bearing assembly, so it was not deemed applicable due to its unique mechanical configuration. It was later restored to the same configuration as the other flight units after a rework/rebuild, so only those data sets were applicable. The investigations focused specifically on: 1) assessing general data trends and consistencies, 2) quantitatively evaluating variability characteristics and factors, and 3) extracting heretofore unknown comparative data on additional harmonics. This last effort was important to assess which harmonics had a significant system-level impact on LOS jitter since it was a challenge to determine the effect based on simple first principles. It should be noted that between each dataset all RWAs are exposed to varying environmental/test conditions (e.g., Random Vibration or Thermal-Vacuum Cycling), so results exhibit effects from both: 1) variations generated by adverse environmental exposures that may alter micro-structural conditions particularly in the bearings-lubrication (i.e., conditions simulating expected launch-to-orbit and/or simulated on-orbit operating conditions), and 2) variations due to low-intensity handling and inherent test-to-test random factors (presumed to be significantly smaller than extreme environment exposures). It is impossible to determine precisely how much IV dataset-to-dataset variation is due to which of these specific causes. However, attempts were made to limit/bound the changes[14].

Investigations applied the following specific methodology sequence to study/filter the large amount of IV data from the 20 data sets comprising over 3700 individual speed-with-magnitude data points total:
1) Accumulate, basic sort, tabulate, and scrutinize all available-viable data; exclude or interpolate-adjust highly-anomalous or significantly out-of-family data measurements (i.e., clear outliers).
2) Evaluate then document preliminary conclusions; founded upon prior jitter analyses results.
3) Compute second-order best-fit-curve coefficients for the amount (sometimes variable) of dataset points and corresponding frequencies for each dataset.
4) Select overall compatible criteria for establishing the "final" curve more-direct comparisons.
5) Compute baseline second-order best-fit-curve coefficients and equivalent geometry error values based on above-chosen criteria/comparisons.
6) Tabulate and graph results; evaluate results and produce consolidated conclusions.

A top-level list of all RWA IV acceptance test datasets (24) and subsets (20) studied are in Table 12. Consolidated tables of detailed dataset values for local RWA directions and harmonics are in Appendix A. Computational results of second-order coefficients and root-mean-square (RMS) errors for best-fit-curves,

387

involving varying numbers of data points (rotation speeds) per curve, for key harmonics are in Tables A-1 to A-5 These tabulations established the foundation for final criteria to evaluate dataset curve differences. Rationale/justification for final selection of axial data points used for comparative evaluation of the four primary harmonics in local axial force, radial force (2), and radial moment (2) directions is in Appendix B. The four harmonics, as discussed above, are sufficient for HST LOS jitter analytical assessments[14].

Table 12. Master Tracking List for All HST RWA Acceptance Tests Containing IV Datasets[14]

RWA No.	Func. Tests Completed	IV Tests Completed	Test Data Name/Designation	Start Date	Data Vol.	Comments	
1001	9	8	1 – First Full Functional	11/26/84	IV	Full IV Set	← Rotor Rebalanced
			2 – First Full Func (Retest)	11/29/84	IV	Full IV Set	
			3 – Post Vibe Abbr. Func.	12/04/84	V	Minimal IV	← Rotor Changed**
			4 – Final Full Functional	12/11/84	VI	Minimal IV	
			5 – Abbreviated Functional	01/06/85	VII	Partial IV Set	
			6 – Abbreviated Functional	01/16/85	VII	Partial IV Set	
			--- Mini-Functional	01/18/85	VIII	No IV Data	
			7 – Abbreviated Functional	01/21/85	VIII	Partial IV Set	
			8 – Final Functional Test	**01/26/85**	**IX**	**Full IV Set**	**[Jitter Baseline]**
1002	4	3	1 – Ambient Functional	12/04/84	IV	Partial IV Set	
			2 – Post Vibe Abbr. Func.	12/07/84	V	Partial IV Set	
			3 – Partial Abbr Func.	02/8/85	V	No IV Data	
			4 – Final Functional Test	**02/13/85**	**VI**	**Full IV Set**	**[Jitter Baseline]**
1003*	4	3	1 – First Functional	01/17/85	Prel.*	Partial IV Set	
			2 – Abbreviated Functional	01/19/85	Prel.*	Partial IV Set	
			3 – Partial Abbrev. Func.	07/08/85	Prel.*	Partial IV Set	
			4 – Final Full Functional	---	---*	---*	
1004	8	6	1 – First Full Functional	09/15/84	IV	Full IV Set	
			2 – Post Vibe Abbr. Func	09/21/84	V	Full IV Set	
			3 – Abbreviated Functional	11/18/84	VI	Partial IV Set	
			4 – Final Full Functional	**11/23/84**	**VII**	**Full IV Set**	**[Jitter Baseline]**
			5 – Short Functional	01/05/85	VIII	No IV Data	
			6 – Final Abbreviated Func.	01/08/85	VIII	Partial IV Set	
			7 – Mini Functional Test	01/18/85	IX	No IV Data	
			8 – Abbreviated Functional	01/21/85	IX	Partial IV Set	
1005	6	4	1 – First Full functional Test	11/25/84	IV	Partial IV Set	
			2 – Post Vibe Abbr. Func.	12/09/84	V	Partial IV Set	
			3 – Short Functional Test	01/05/85	V	No IV Data	
			4 – Final Functional Test	**01/13/85**	**VI**	**Full IV Set**	**[Jitter Baseline]**
			5 – Short Functional Test	01/19/85	VII	No IV Data	
			6 – Abbreviated Functional	01/23/85	VII	Partial IV Set	

*   Data not yet completed and officially delivered by final compilation/reporting.
**   RWA 1001 prior IV data collected non-compliant and not consistent with final rotor flight configuration.

General and Specific Findings Derived from Detailed Investigations of Compiled RWA IV Test Data

Evaluation of compiled IV data resulted in these findings (ordered roughly from general to more specific):
1) IV datasets generally show expected consistency, and reconfirms the fact that all flight-accepted RWAs met specification limits with no evidence of systematic test errors or glaring discrepancies.

2) Most variations in each RWA's data/test-to-test differences seem to be related to test apparatus/data-gathering/data-processing/handling variances/limitations versus definitive trends that clearly indicate a detectable physical change within the RWA unit.

3) Clearly notable anomalous data points are rare (<~1%), and appears that the supplier's computer processing program that selects peak values for harmonics is generally functioning as-expected.

4) Significant test data variances are observed in higher harmonics at RWA rotational speeds that place the harmonic in proximity to the known rotor-housing resonance passage frequency.

5) Four primary axial harmonics (1.0, 2.0, 2.8, and 5.2) generally provide sufficient data for valid set-to-set comparative evaluations: other axial harmonics were either unreliable criteria (e.g., 0.35), or provide too few data points in the range of interest for conclusive evaluation (5.6, 7.5, and 8.5).

6) There is no evidence of a strong correlation between overall noise data and stage-of-acceptance testing or retesting; however, the first set of data (obtained immediately after mechanical build-up, checks, and fine-rebalancing) tends to be one of the quieter sets for any individual RWA.

7) There is no evidence of strong correlation between final rotor unbalance level (indicated by radial force 1.0 harmonic) and overall RWA noise output/jitter (indicated by four key axial harmonics).

8) General correlation exists between radial force and radial moment IV for the 4 key harmonics.

9) Data obtained near any harmonic's passage of the RWA's internal natural resonance (~85-90 Hz) is commonly highly inconsistent from dataset to dataset; also, data for other harmonics not near the resonance range can regularly show abnormal variation due to the influence of the harmonic-passage phenomenon (another harmonic), so should always be checked for validity/outlier status.

10) The qualitatively noisiest overall dataset appears to be set #5 on RWA 1004; quietest overall dataset appears to be set #1 or #3 on RWA 1003.

11) The most "typical" dataset recommended for preliminary jitter assessment for RWA 1003 is #3.

12) The RWA 1004 2.0 harmonic data (all DOFs) is consistently abnormally low (no known reason); speculation is inordinately small values for imperfection in runout(s) and bearing cage roundness.

13) Overall qualitative noise rankings for HST RWAs (ordered noisiest to quietest) are:

Ranked by Force Unbalance [1.0 Radial Harmonic]	Ranked by Overall Noise Output [Using 4 Key Axial Harmonics]
1) 1005	1) Tie – 1001
2) 1003	1) Tie – 1005
3) 1001	3) 1002
4) 1002	4) Tie – 1004
5) 1004	4) Tie – 1003

14) Datasets chosen for most-representative-but-not-overly-quiet (therefore as-tested, but leaning to normal-to-high noise variance) baseline HST jitter predictions (e.g., investigations for isolation properties studies) are #4 (1001), #3 (1002), #4 (1004), and #3 (1005); all are full datasets from last full functional acceptance test runs, and have the following qualitative validity assessments:

- 1001 – no clear trend; 1.0 and 2.8 harmonics tend low, while 2.0 and 5.2 tend high.
- 1002 – tends to be somewhat higher values overall than average 1002 dataset
- 1004 – typical dataset
- 1005 – typical dataset

Orbital IV Structural Dynamic Predictive Capability Evaluations and Results Confirmation

As discussed above, HST ground modal test investigations, via a suspended (stowed configuration) with flight-like units plus mass simulators substituted for some equipment boxes/modules, confirmed excellent correlation between data and pretest analytical results for structural mode frequencies, mode shapes / transmissibilities, damping, and predicted known-source responses. Findings validated models required for dynamic load/clearance requirement verification (i.e., launch and ascent) and jitter evaluation (deployed configuration not practical to realistically ground test). Although a recommended Lockheed plan was put forth enabling on-orbit measurements (e.g., using a minimal set of accelerometers, largely based on already-installed ground test instrumentation) to verify HST dynamics and jitter performance, NASA chose to not fund such efforts. The decision was predicated upon a low and acceptable risk assessment; wherein existing evidence supports that all on-orbit disturbances are identified, accounted for, worst-case bounded,

and met system requirements (with margin). However, with the unexpected on-orbit discovery of a thermal-change-induced sudden energy release causing the PCS performance to fail requirements, alternate forensics were improvised to check suspected source(s) and the nature of the phenomenon[17]. The only onboard sensors deemed sensitive enough to obtain dynamic data were gyros, HST-designated Rate Sensor Units (RSUs). RSU telemetry, along with the correlated dynamics allowed the root cause to be well-correlated with other data (e.g., via event timing and which known mode frequencies are excited by the phenomenon plus what disturbance locations are likely to excite particular modal responses) and eventually traced to locations within the 2 solar arrays. Extremely flexible when deployed (due to weight-optimized design), solar arrays with extended bi-stem supports were expected to slowly deform when reacting to thermal changes transitioning through terminator crossings from orbital day to night. However, it was discovered instead that one solar array would "lock-up" for some time then abruptly snap into a different bowed position. This sudden impulse was sufficient to cause FGSs to lose interferometric lock on designated guide stars reverting to coarse-sensing mode and typically resulting in a loss of science. The ensuing investigation found a documented history of orbital disturbances occurring during transitions from orbital day-to-night (EOD) and night-to-day (EON), plus near-steady-state conditions during middle of orbit day (MIDD) and middle of orbit night (MIDN)[17]. RSU telemetry data sensing vehicle rotational rate changes were extensively measured under these conditions, and these data proved useful in computing linear accelerations experienced on the spacecraft at given distances from the HST center-of-gravity[18].

These established capabilities allowed, for the first time, an opportunity to confirm other orbital dynamic jitter-related predictions thereby, also opening an applicability to other large space platform microgravity predictive approaches[4,12]. Subsequently, a unique analytical effort was initiated to compute HST structural dynamic responses (accelerations) due to prescribed input forces/moments substantiated with actual on-orbit telemetry measurements for a specific known input disturber propagating through proven HST dynamics to a sufficiently sensitive and known output receiver. Although RWA IV input levels were well-established due to earlier efforts described, viable direct orbital response results for RWAs was not practical due to several pragmatic issues: 1) as researched, ground-to-orbit RWA IV variability could be substantial and non-deterministic[14] (i.e., although it had been bounded, it could not be precisely known within that range what long-term IV level was present on any given RWA at a particular time), 2) telemetry acquisition data rates were not high enough to readily resolve key high-harmonic-ratio signal components (one of the factors supporting the earlier decision to not pursue on-orbit jitter verification), 3) on-orbit RWA rotational rates where telemetry was most available during HST science acquisition tended to be near the lowest values of pre-launch predictions (typically 0-3 Hz) which resulted in inherently very low RWA IV disturbance levels, 4) effective vibration isolation highly suppressed RWA IV[9], and, lastly (due largely to such low IV levels from 3 and 4), 5) HST telemetry data had never detected nor distinctly identified a response clearly due to RWA IV frequency inputs above general on-orbit operational noise environments. However, upon further investigation, an alternative disturbance source was found allowing a highly reliable/consistent on-orbit basis for an analytical approach: Engineering/Science Tape Recorders (ESTRs). HST's ESTRs (2 onboard for redundancy) countered RWA impediments by having consistent IV-to-response knowledge: 1) highly repeatable ground test IV data showing no basis for significant variability transitioning to orbit or due to changing conditions (e.g., designed for similar performance independent of overall tape position/condition, i.e., start-of-reel/end-of-reel), 2) time-congruent telemetry available (at 2 different disturbance frequencies matching 2 stable ESTR recording rates), 3) telemetry data uniformly exhibits a dominant and unambiguous signal presence when an ESTR is on, and 4) source and receiver have distinct local orthogonal principal directions (corresponding to the ESTR input IV known dataset directions and RSU output dynamic model along with sensed response directions (i.e., no need for a coupled coordinate transformation of amplitude caused by difficulty in discerning which response directions' signal intensity was from which individual disturbance DOF). Specifically, the local primary spin axis of ESTR tape reels is coincident with the vehicle V1 axis which is also accurately aligned with one of the principal RSU sensing axes - a favorable situation.

As measured, RSU angular acceleration telemetry signals encompassed all operating onboard sources up to 20 Hz, including solar array residual motions, ESTRs, High Gain Antenna Gimbals, etc. To isolate ESTR-only contributions, a filter was applied since the effective frequency bandwidth is reliably known (quite

narrow for ESTR). An ESTR has a precise frequency output during slow-speed recording at 1.375 Hz; repeatedly reconfirmed in on-orbit tests[18,19]. Telemetry data are bandpass filtered (1.1-1.5 Hz) via a Blackman window for each principal HST axis (V1, V2, and V3). Bandpass rates are then differentiated for each Solar Array orbital event type, producing RSU angular accelerations. Results are multiplied by the distance to the HST C.G. to obtain an equivalent local linear acceleration at 3 specific locations. Root-mean-squared (RMS) values (over time) are then computed for each orbital disturbance period. As a specific reference, worst-case-maximum computed acceleration for the known ESTR input primary frequency (i.e., 41 inches-per-second recording rate) is 0.75 µg (axially) and 0.49 µg (radially).

Once the on-orbit model is correlated for the ESTR known reference source, RWA inputs are applied. Since ground-to-orbit additive RWA IV variability cannot be known with certainty, worst-case as-tested IV forces and moments (with 4 key harmonic ratios; 1.0, 2.0, 2.8, and 5.6) define input amplitudes; derived from computed coefficients[14]. Periodic (i.e., pure sinusoidal) time histories are created for each RWA harmonic for 2 different rotation rates: 3 Hz (nominal on-orbit maximum) and 10 Hz (typical-4-wheel case/condition upper bound). Individual time histories for the 4 key harmonics are combined by direct addition, no time-phasing nor dithering is done to simulate random phasing. Time histories are combined simultaneously at an RWA rotor source (for all local DOFs) in the HST on-orbit dynamic FEM. Resulting frequency-domain response, i.e., Fast-Fourier Transforms (FFTs), are developed; 2 typical input-output examples (10 Hz RWA) of response at the SSM Equipment Bay (EB) (V2 direction) and RSU (V1 direction) are shown in Figure 11[20]. Note dominant modal (i.e., non-optical here) transmissibilities at 10, 20, 28, and 52 Hz: isolation system damped resonances are present. Also note that, summed results are primarily dominated by rigid body responses to the set force/moment RWA inputs, with the additive structural response being minimal (further confirmation that the RWA isolation system is performing as intended). Summary HST results are listed in Tables 13 and 14. Note that this was a first on-orbit reference confirmation leading to the level of challenge presented in attaining low microgravity limits for the International Space Station[12].
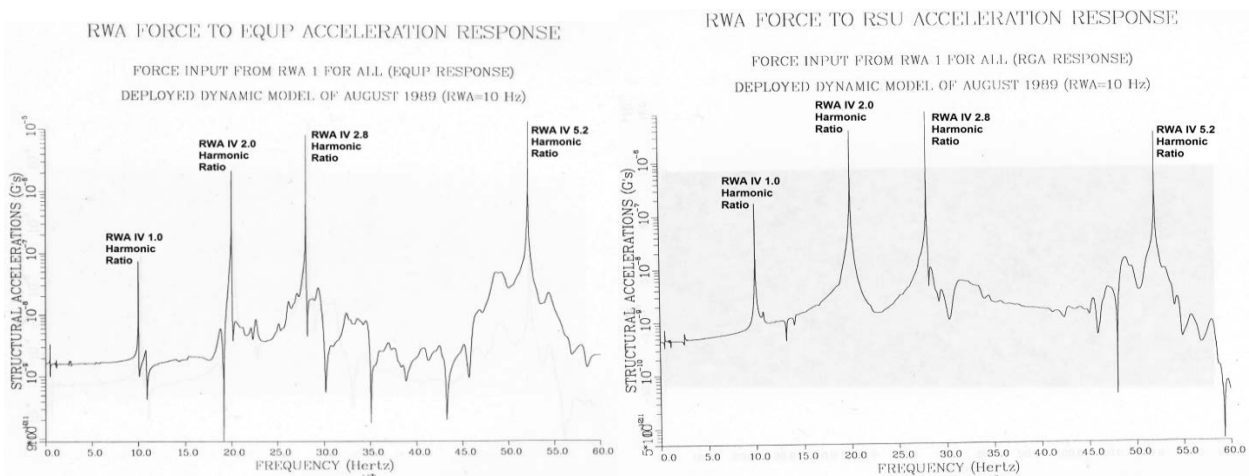
Figure 11. HST Microgravity-Related Acceleration Response - Examples at EB (V2) & RSU (V1)[20]

Table 13. HST On-Orbit Acceleration Results; ESTR 1.375 Hz Input during Solar Array Transitions (4)[20]

HST Prin. Direction	EON Event	MIDN Settling	EOD Event	MIDD Settling
V1$_{RMS}$	0.49 µg	0.49 µg	0.66 µg	0.65 µg
V2$_{RMS}$	0.03 µg	0.02 µg	0.04 µg	0.02 µg
V3$_{RMS}$	0.09 µg	0.05 µg	0.12 µg	0.05 µg

Table 14. HST On-Orbit Acceleration Results; RWA Primary Harmonic (4) Inputs-to-HST Locations (3)[20]

HST Prin. Direction	Forward	Equip.	RSU Near
Distance from HST C.G. →	194 inches	57.2 inches	81.3 inches
RWA Speed = 3 Hz (180 RPM)	-	-	-
$V1_{RMS}$	0.08 µg	0.18 µg	0.10 µg
$V2_{RMS}$	0.33 µg	0.30 µg	0.11 µg
$V3_{RMS}$	0.05 µg	0.49 µg	0.08 µg
RWA Speed = 10 Hz (600 RPM)	-	-	-
$V1_{RMS}$	4.45 µg	8.17 µg	7.76 µg
$V2_{RMS}$	8.62 µg	13.23 µg	5.63 µg
$V3_{RMS}$	5.44 µg	3.41 µg	7.24 µg

Systems Engineering (SE) Introduction/Overview for Basic RWA Sizing and Affordability for Jitter

Looking ahead to future uses and affordability issues, spacecraft SE RWA choices for jitter-performance-versus-cost prompts many considerations. Because 1) costs are critical overall program drivers, 2), ACS/GN&C subsystems are a notable contributor to satellite costs, 3) RWAs are an essential stabilized spacecraft need, 4) RWAs are, on a mass-sizing basis, one of the more costly single components, 5) supplier alternatives are a relatively small set of options to push for competitively lower pricing, and 6) cost-performance trades are a basic system engineering tool to d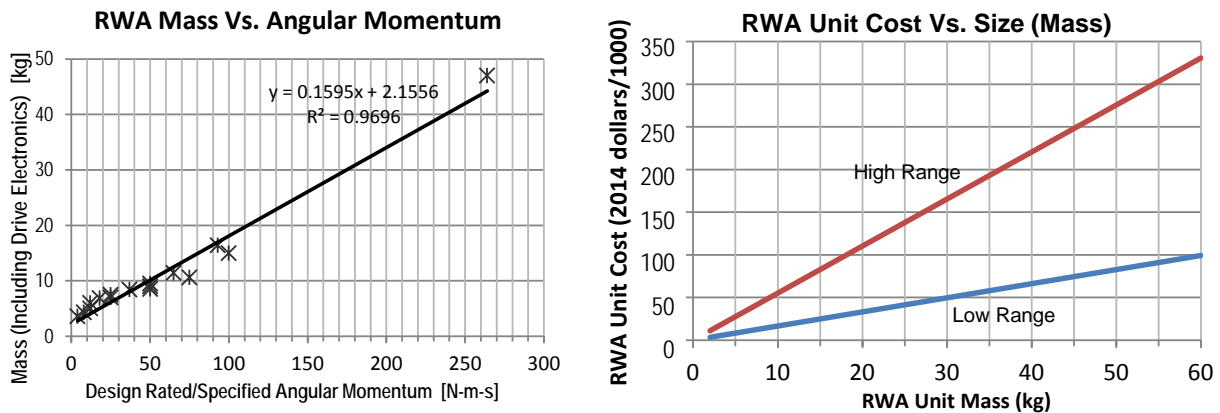etermine component selection, there is a need for quantitative cost evaluations. To a first order, RWAs are chosen (allowing for adequate margins in power, mass, angular momentum, etc.) as small as possible via two key values: 1) spacecraft size (i.e., maximum spin-axis-control inertia), and 2) maximum required slew rate. However, considering stringent jitter limits, RWA tradeoffs become more complex. Smaller RWAs otherwise capable of the basic station-keeping/pointing mission commonly have several inherent deleterious impacts: 1) smaller RWA designs have smaller parts (i.e., bearing components and reduced dimensions) that impact efforts to keep tolerances low (without other compensating efforts) and raise harmonic ratios' frequencies (i.e., see prior 304H-vs-101H), 2) smaller RWA mass lowers local reaction mass for mitigating prime IV disturbance energies originating at bearing imperfections, 3) higher spin speeds for a target angular momentum value forces IV amplitudes (i.e., non-spin-axis harmonics) to increase significantly (i.e., by speed squared) that also drives more responsive transmissibilities, and 4) smaller rotor fine-balance adjustments are often more challenging. A seemingly straightforward more-affordable choice for minimal-size RWAs, with upfront acquisition cost savings, can actually translate to *higher* final cost to attain and successfully verify IV limits. Figure 12 shows NASA-mission subsystem percentage costs and similar relationships for other large satellites[21,22]. Note that, very generally, atypical elements of NASA's widely-varied missions (planetary landings/fly-bys, manned space, solar monitoring, etc.) can drive more complex orbital mechanics/GN&C rather than RWA costs compared to GEO satellite platforms driven by station-keeping commonalities, e.g., normal transfer-to-orbit plus pointing stability. Although a complex military satellite program can drive costs from roughly three to eight times higher than basic commercial/NASA missions due to demanding requirements (reliability, threat hardening, etc.), proportions shown in Figure 12 are roughly scalable and percentages are representative. Note that ACS is non-trivial: typically of the order of 5-8% of mission costs[21,22].

Average NASA small satellite mission	
Total mission cost	$145M
Mission development time	3 years
Dry Mass	407 kg.
Spacecraft bus cost	41% TMC

Larger Satellites
[Up To Several Tons Mass (15)]

Key: Payload ▨ Structure ☐ TCS ☐ EPS ⊞ TT&C ☐ ADC/ACS ☐ Propulsion

Figure 12: General (Scalable) Cost Proportions for Typical NASA Spacecraft and Large Satellite System-Missions[21,22].
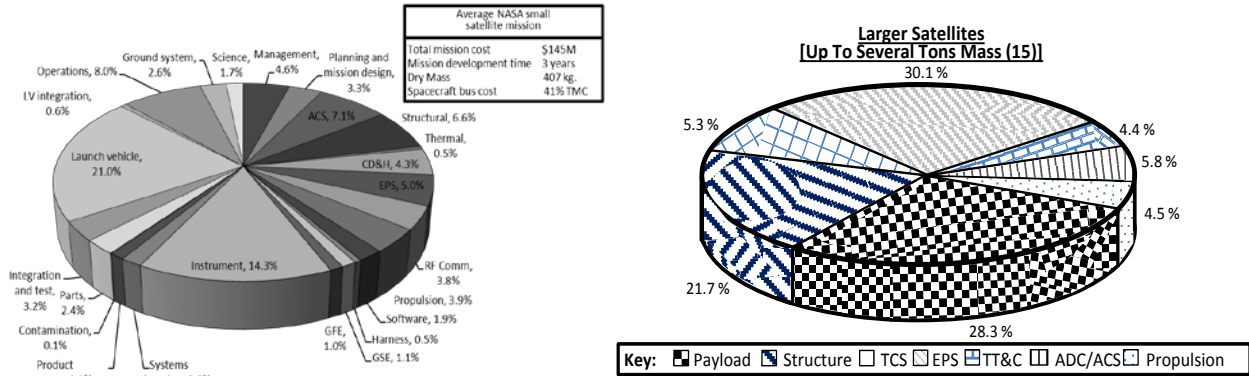
Estimated ACS-related costs have limited utility unless the scope (i.e., actual size) of a particular RWA unit is better quantified. An established tool for SE parametric cost analysis applies multiple-program data to create Cost Estimating Relationships (CERs) for the size/performance needed and historical known-costs (adding development-related factors). RWA CER equations have been determined, however, they depend on unit mass, whereas per-axis maximum angular momentum capability drives basic tradeoffs. Therefore, as a bridge, a relationship between mass and angular momentum is established (with good overall correlation)[22,23]. Note that this relationship encompasses RWAs from ~3-300 kg, so is relevant for medium-to-large satellites, but needs revision for micro/small-sat applications[24]. To assess future capabilities, the connection from RWA angular momentum to mass to CER (Figure 13) was validated by comparisons with recent (circa 2014) known inertia wheel procurement costs to substantiate lower and high bounds; cost analysis sources show an RWA range of roughly 1.5-5.0% of satellite procurement costs[25], a typical range for RWA per-set costs are approximately 3-4% of overall satellite procurement costs[26].

RWA Mass Vs. Angular Momentum

$y = 0.1595x + 2.1556$
$R^2 = 0.9696$

RWA Unit Cost Vs. Size (Mass)

High Range

Low Range

Figure 13. RWA Angular Momentum Sizing & Cost-Estimating-Relationship Projection[22,23,24,25]

Note that a wide variety of programmatic factors (e.g., small or singular procurements, design qualification for a particular mission-environments, quality control-related requirements, special testing, added documentation and particular added program requirements, etc.) raises costs: higher range/limit of values. Alternately, larger contract buys (often an impediment with high-performance spacecraft), minimal testing, minimal documentation, and low procurement overhead can drive costs towards lower bounds.

393

RWA IV Data Study Conclusions

Executive-Level RWA IV Study Conclusions:
Based on these overall assessments, summary conclusions for state-of-the-art RWA IV values are (note that, although not rigorously quantified, the values given are intended to represent ~2-sigma variation):
- Test-to-test amplitude is generally within ~±35% of the average dataset value for a specific RWA.
- There is no evidence of large (e.g., ~3-sigma) RWA-to-RWA mechanical noise/jitter variations if all are otherwise flight-acceptable/spec-compliant, no out-of-family/trending/anomalous RWA quality issues.
- IV LOS jitter analytical result variation for ambient-test-to-nominal-orbit-condition transitions is approximately ±25% for average RMS values and ±50% for peak RMS values.
- IV LOS jitter analytical result variation factor for ambient-test-to-worst-orbit-condition-transitions is approximately ±50% for average RMS values and ±100% for peak RMS values.

Specific RWA IV Study Insights/Conclusions:
Based on the foregoing evaluations and detailed investigations, the following detailed conclusions result:
- Qualitative analysis and review of IV datasets substantiate their validity and confirmed in this study effort basic tenets of RWA bearing-rotor construction, imperfections, and first-order physics.
- IV testing dataset variations, including both test-to-test and environmental-exposure variations, for key (linked) 2.8 and 5.2 axial-direction harmonics show 1-sigma variances of approximately ±0.6 and ±0.3 µinch (±0.015 and ±0.007 µm) equivalent geometry error respectively: equating to ~±35% variance on the all-RWA average value(s). [Ref. Ap. A tabular data]
- IV testing data set variations, including both test-to-test and environmental-exposure variations, for key (linked) 1.0 and 2.0 radial-direction harmonics show 1-sigma variances of approximately ±2.0 and ±0.4 µinch (±0.50 and ±0.10 µm) equivalent geometry error respectively: equating to ~±35% variance on the all-RWA average value(s). [Ref. Ap. A tabular data]
- Total combined (via RSS summing) expected variations due to transition from ground to nominal and extreme orbital environment conditions in axial and radial direction 1.0 harmonics have the largest test data basis; accounting for variations of roughly ±1.5 and ±3.0 µinch (±0.04 and ±0.08 µm) equivalent geometry error respectively: equating to ~±20% and ~±40% variance on the all-RWA average value(s). [Ref. Ap. A tabular data]
- Total combined (via RSS summing) expected variations due to transition from ground to nominal and extreme orbital environment conditions in other-direction higher key harmonics are not well known/characterized and speculative, but are estimated to account for variations of roughly ±0.8 and ±1.5 µinch (±0.02 and ±0.04 µm) equivalent geometry error respectively: equating to ~±25% and ~±50% variance on the all-RWA average value(s). [Ref. Ap. A tables]
- HST RWA LOS jitter analytical results variability estimate for ambient-to-nominal-orbit-condition transitions correspond to 0.74 to 1.16 milli-arcsecond average RMS values and 4.54 to 10.22 milli-arcsecond for peak RMS values for the overall noisiest-worst-case RWA dataset (1005).
- HST RWA LOS jitter analytical results variability estimate for ambient-to-extreme-limit-orbit-condition transitions correspond to 0.62 to 1.40 milli-arcsecond average RMS values and 3.41 to 13.63 milli-arcsecond for peak RMS values for the overall noisiest-worst-case RWA dataset (1005).
- Additional RWA harmonics should be evaluated in overall jitter analyses, depending upon general system fidelity required and engineering judgment on a potential for high frequency disturbances to affect optical train elements. [Ref. Ap. A tables for comparison of relative harmonic magnitudes]

Summary

A RWA IV jitter optimization treatise, focused on an ultra-fine-pointing spacecraft utilizing state-of-the-art RWA IV balancing/measurements along with system engineering aggregated efforts, is documented. Key findings, methodologies, overviews, and intertwined details for lower-level elements within HST's design-test-analysis evolution, commonly with nuanced discoveries and counter-intuitive paradigm shifts in approaches and resolution path, are summarily discussed often within a background/historical context. However, a clear focus is also maintained on how these multiple dependencies contribute to present and

future LOS-pointing satellite developments, as well as how they translate to other spacecraft units with a potentially deleterious IV signature, e.g., rotating or dithering components, etc. From a global viewpoint, it can seem difficult to see how a few-ounce miniscule part's (i.e., RWA bearing raceway/retainer) barely measurable imperfections can amplify into a formidable challenge for a ~12-ton spacecraft's primary LOS jitter allocations under unfavorable conditions. Although not common for most satellites to engage all of these approach details, attainment and prudent management of lower-level IV data is essential for fine-pointing space platform's success. This paper's predominant value is in exposing both applicability guidance plus revealing insights/means to pursue in-depth key details to attain fine-pointing requirements.

References

1. Dougherty, H. J., Rodoni, C., Rodden, J., Tompetrini, K., "Space Telescope Pointing Control", AAS/AIAA Paper 83-365, Astrodynamics, Vol 54 1 & 11, Advances In The Aeronautical Sciences, 1983.
2. Beals, G. A., Crum, R. C., Dougherty, Hegal, D. K., Kelley, J. K., Rodden, J. J., "Space Telescope Precision Pointing Control System", AIAA Technical Paper 86-1981, AIAA Guidance, Navigation, and Control Conference Proceedings, 1986.
3. Beals, G. A., "Hubble Space Telescope Pointing Control Subsystem Error Budget Report," LMSS Report D977241A, Lockheed Martin Space Systems Company, Sunnyvale, California, August 1989.
4. Hasha, M., A. Blackwell, L. Chang, G. Sarver, "Facility Vibration Limits in Micro-gravity and Low-gravity Environments: An Allocation Methodology", AIAA 35th Aerospace Science Sciences Meeting, Accelerations and Countermeasures in the Reduced Gravity Environment Session, Reno, NV, 1997.
5. Kendrick, S. E., Stober, J., Gravseth, I., "Pointing and Image Stability for Spaceborne Sensors – from comet impactors to observations of extrasolar planets" SPIE Journal Vol 6265, 62652V-1, 2006.
6. Dougherty, H. J., Rossini, R., Simcox, D., Bennett, N., "Space Telescope Control System Science User Operations", AAS/AIAA Astrodynamics Specialist Conference, Lake Placid, NY, August 1983.
7. Hur-Diaz, S., Wirzburger, J., Smith D., "Three Axis Control of the Hubble Space Telescope Using Two Reaction Wheels and Magnetic Torquer Bars For Science Observations", AAS 08-279, F. Landis Markley Astronautics Symposium, June 2008.
8. Rodden, J., H. Dougherty, F. Reshke, M. Hasha, and P. Davis, "Line of Sight Performance Improvement with Reaction Wheel Isolation", AAS Pub. 86-005 Guidance and Control Conference, Keystone, CO, Feb 1-5, 1986.
9. Hasha, M., "Passive Isolation/Damping System for the Hubble Space Telescope Reaction Wheels", NASA Conf. Pub. 2470 21st Aerospace Mechanisms Symposium, NASA-JPL-LMSC, Houston, TX, Apr 29-May 1, 1987 [Recipient of George Herzl Award for Best Technical Paper].
10. Launius, Roger D., DeVorkin, David, "Hubble's Legacy: Reflections by Those Who Dreamed It, Built It, and Observed the Universe with It", Smithsonian Proceedings and Other Publications, 2014.
11. Hasha, M. D. "SSM Stowed Dynamic Model of February 1983", Engineering Memorandum S&M 357, LMSC, June 1983.
12. Hasha, M., "Compatibility of the Space Station Freedom Life Sciences Research Centrifuge with Microgravity Requirements", ASME Conf. Pub. 90-WA/AERO-6 Winter Annual Meeting, Dallas, TX, Nov 25-30, 1990.
13. Hasha, M. and J. Hirata, "SOFIA Telescope Assembly Jitter Reduction Using Advanced Passive Isolators", AIAA 33rd Aerospace Sciences Meeting, Space Sciences and Astronomy Session, Reno, NV, Jan 9-12, 1995.
14. Hasha, M. D., "Reaction Wheel Mechanical Noise Variations," Engineering Memorandum SSS 218, LMSC, June 1986; which includes Ross, G., Hasha, M. D., plus "Applicability of Key Harmonics For Predicting Reaction Wheel Jitter Trends", Internal Communication Report, LMSC, 11 September 1985.
15. BRÜEL and KJAER, "Static and Dynamic Balancing of Rigid Rotors", Application Notes, Germany, Naerum Offset, 1989.
16. Mauriello, J. A., et al., "Rolling Element Bearing Retainer Analysis", Army Air Mobility Research and Development Laboratory Publication AD-774 264, November 1973.
17. Lallo, M. D., "Experience with the Hubble Space Telescope: Twenty Years of an Archetype", Cornell University Library/Space Telescope Science Institute Publication, 2012.

18. Camino, T. S., "HST Solar Array Feathering Test II Test Report", Engineering Memorandum SPS 648, LMSC, July 1991.
19. Camino, T. S., Hasha M. D., "Structural G Level Accelerations at 1.0 and 100.0 inches from CG of HST during Solar Array Feathering Test II to be used as a Demonstration for Space Station", Engineering Memo Communication, September 1991.
20. Sills, J. W., Hasha, M. D., "Derived Structural Accelerations for the HST Due to Reaction Wheel Harmonic Steady State Inputs and Engineering/Science Tape Recorders Telemetry Data, Interdepartmental Communication Report, LMSC, 16 September 1991.
21. Guerra, Lisa, "Cost Estimating Module – Space Systems Engineering Version 1.0", Course Materials Developed under NASA Exploration Systems Mission Directorate in association with the University of Texas at Austin, 2010.
22. Aas, C., Zandbergen, B.T.C. , Hamann, R.J., Gill, E.K.A., "SCALES – A System Level Tool for Conceptual Design of Nano- and Microsatellites", 7th IAA Symposium on Small Satellites for Earth Observation, Berlin, Germany, May 4-8, 2009.
23. Larson, W.J., Wertz, J.R., "Space Mission Analysis and Design" or "SMAD", 3rd Ed., Microcosm Press & Springer, 1999.
24. Aas, C. L. O., Zandbergen, B. T. C. , Hamann, R.J., Gill, E .K. A., "Development of a System Level Tool for Conceptual Design of Small Satellites", 7th Annual Conference on Systems Engineering research 2009 (CSER 2009), April 20-23, 2009.
25. Aerospace Corp. Small Satellite Cost Model Ver 7.4, CER via www.coursehero.com\Georgia State/ASTR\ASTR 6300 [homework 7 - page 4 of 13].
26. Comparisons with Internal Engineering Assessments, Internal Guidelines Discussion between D. Anderson and M. Hasha, September 1, 2015.

Appendix A: Consolidated Specific Details for RWA IV Dataset Values

Table A-1. Computed Values for RWA Axial Force Principal Direction Key Harmonics (4)

Data Set	1.0 Harmonic		2.0 Harmonic		2.8 Harmonic		5.2 Harmonic	
RWA S/N - Set	2nd-O Coef (mlb/RPM^2)*	Eq. GE (µin)	2nd-O Coef (mlb/RPM^2)*	Eq. GE (µin)	2nd-O Coef (mlb/RPM^2)*	Eq. GE (µin)	2nd-O Coef (mlb/RPM^2)*	Eq. GE (µin)
1001 – 1 (P)	9.22	7.58	7.40	1.52	19.53	2.02	28.80	0.88
1001 – 2 (P)	7.99	6.56	9.17	1.88	23.44	2.42	31.86	0.98
1001 – 3 (P)	6.65	5.46	9.13	1.87	16.83	1.74	35.68	1.09
1001 – 4 (F)	6.73	5.53	8.86	1.82	16.14	1.67	34.49	1.06
1001 – ave.	7.65	6.28	8.64	1.77	18.98	1.96	32.71	1.00
1002 – 1 (P)	1.11	0.91	1.97	0.40	15.33	1.58	26.71	0.82
1002 – 2 (P)	0.74	0.61	6.17	1.27	19.39	2.00	33.31	1.02
1002 – 3 (F)	2.26	1.85	6.78	1.39	18.18	1.88	37.68	1.15
1002 – ave.	1.37	1.12	4.97	1.02	17.64	1.82	32.57	1.00
1003 – 1 (P)	4.07	3.35	3.45	0.71	6.91	0.71	16.79	0.51
1003 – 2 (P)	3.50	2.87	10.40	2.14	24.16	2.50	18.92	0.58
1003 – 3 (P)	2.91	2.39	8.12	1.67	16.50	1.70	6.21	0.19
1003 – ave.	3.49	2.87	7.32	1.50	15.86	1.64	13.98	0.43
1004 – 1 (F)	1.57	1.29	2.73	0.56	17.60	1.82	17.77	0.54
1004 – 2 (F)	2.09	1.72	0.11	0.02	9.00	0.93	15.43	0.47
1004 – 3 (P)	2.35	1.93	0.74	0.15	16.36	1.69	19.92	0.61
1004 – 4 (F)	2.48	2.03	0.43	0.09	15.10	1.56	22.38	0.69
1004 – 5 (P)	4.22	3.47	0.21	0.04	26.38	2.73	37.47	1.15
1004 – 6 (P)	2.29	1.88	0.13	0.03	15.51	1.60	18.62	0.57
1004 – ave.	2.50	2.05	0.72	0.15	16.66	1.72	21.93	0.67
1005 – 1 (P)	3.46	2.84	13.65	2.80	21.13	2.18	19.29	0.59
1005 – 2 (P)	4.32	3.55	8.53	1.75	29.91	3.09	20.72	0.63
1005 – 3 (F)	4.02	3.30	8.17	1.68	30.92	3.19	19.69	0.60
1005 – 4 (P)	4.16	3.42	6.82	1.40	27.74	2.87	21.57	0.66
1005 – ave.	3.99	3.28	9.29	1.91	27.43	2.83	20.32	0.62
ALL – ave.	3.81	3.13	5.65	1.16	19.30	1.99	24.17	0.74

* Note: all milli-pound/RPM^2 values shown are 10^6 times actual values for tabulation clarity.

Table A-2: Computed Values for RWA Radial Force Principal Direction Key Harmonics (4)

Data Set	1.0 Harmonic		2.0 Harmonic		2.8 Harmonic		5.2 Harmonic	
RWA S/N - Set	2nd-O Coef (mlb/RPM^2)*	Eq. GE (µin)	2nd-O Coef (mlb/RPM^2)*	Eq. GE (µin)	2nd-O Coef (mlb/RPM^2)*	Eq. GE (µin)	2nd-O Coef (mlb/RPM^2)*	Eq. GE (µin)
1001 – 1 (P)	8.56	7.04	7.67	1.57	13.89	1.43	7.90	0.24
1001 – 2 (P)	7.96	6.54	2.42	0.50	9.78	1.01	3.31	0.10
1001 – 3 (P)	9.73	8.00	5.65	1.16	12.41	1.28	10.07	0.31
1001 – 4 (F)	9.11	7.48	4.11	0.84	10.81	1.12	7.89	0.24
1001 – ave.	8.84	7.26	4.96	1.02	11.72	1.21	7.29	0.22
1002 – 1 (P)	4.23	3.47	3.69	0.76	7.52	0.78	6.76	0.21
1002 – 2 (P)	5.76	4.73	4.58	0.94	5.93	0.61	6.26	0.19
1002 – 3 (F)	11.59	9.52	3.94	0.81	6.28	0.65	6.40	0.20
1002 – ave.	7.19	5.91	4.07	0.84	6.58	0.68	6.48	0.20
1003 – 1 (P)	14.43	11.86	5.59	1.15	9.26	0.96	3.66	0.11

Data Set								
1003 – 2 (P)	12.05	9.90	7.85	1.61	9.05	0.93	3.13	0.10
1003 – 3 (P)	11.54	9.48	10.51	2.16	9.55	0.99	4.28	0.13
1003 – ave.	12.67	10.41	7.98	1.64	9.29	0.96	3.69	0.11
1004 – 1 (F)	4.47	3.67	2.74	0.56	7.25	0.75	2.03	0.06
1004 – 2 (F)	4.32	3.55	4.08	0.84	11.17	1.15	5.38	0.16
1004 – 3 (P)	3.11	2.55	4.29	0.88	9.67	1.00	4.25	0.13
1004 – 4 (F)	5.12	4.20	4.42	0.91	7.71	0.80	3.41	0.10
1004 – 5 (P)	4.97	4.08	4.13	0.85	12.25	1.27	4.79	0.15
1004 – 6 (P)	5.92	4.86	4.41	0.91	6.86	0.71	2.45	0.07
1004 – ave.	4.65	3.42	4.01	0.82	9.15	0.95	3.72	0.11
1005 – 1 (P)	14.00	11.50	6.29	1.29	10.52	1.09	3.72	0.11
1005 – 2 (P)	16.05	13.19	5.60	1.15	28.47	2.94	12.17	0.37
1005 – 3 (F)	19.26	15.82	3.49	0.72	12.07	1.25	2.59	0.08
1005 – 4 (P)	15.33	12.59	3.27	0.67	11.08	1.14	6.25	0.19
1005 – ave.	16.16	13.28	4.66	0.96	15.53	1.60	6.18	0.19
ALL – ave.	9.38	7.70	4.94	1.01	10.58	1.09	5.34	0.16

* Note: all milli-pound/RPM^2 values shown are 10^6 times actual values for tabulation clarity.

Table A-3. Computed Values for RWA Radial Moment Principal Direction Key Harmonics (4)

Data Set	1.0 Harmonic		2.0 Harmonic		2.8 Harmonic		5.2 Harmonic	
RWA S/N - Set	2nd-O Coef (mlb/RPM^2)*	Eq. GE** (µin)	2nd-O Coef (mlb/RPM^2)*	Eq. GE** (µin)	2nd-O Coef (mlb/RPM^2)*	Eq. GE** (µin)	2nd-O Coef (mlb/RPM^2)*	Eq. GE** (µin)
1001 – 1 (P)	0.76	6.23	3.60	7.40	15.91	26.43	43.06	13.18
1001 – 2 (P)	1.34	11.01	3.83	7.86	21.92	22.65	36.61	11.21
1001 – 3 (P)	1.97	16.14	4.00	8.21	14.78	15.26	71.85	22.00
1001 – 4 (F)	3.10	25.51	2.49	5.11	20.08	20.74	104.23	31.91
1001 – ave.	1.79	14.72	3.48	7.15	18.17	18.77	63.94	19.58
1002 – 1 (P)	1.14	9.36	2.01	4.14	18.23	18.83	14.82	4.54
1002 – 2 (P)	1.95	16.02	2.13	4.37	14.61	15.10	35.26	10.79
1002 – 3 (F)	8.41	69.13	0.93	1.91	15.98	16.51	15.14	4.63
1002 – ave.	3.83	31.50	1.69	3.47	16.27	16.81	21.74	6.66
1003 – 1 (P)	8.10	66.54	5.23	10.74	18.91	19.53	31.67	9.70
1003 – 2 (P)	7.46	61.25	4.82	9.89	19.73	20.38	44.98	13.77
1003 – 3 (P)	6.85	56.30	24.45	50.21	23.46	24.23	18.16	5.56
1003 – ave.	7.47	61.36	11.50	23.62	20.70	21.38	31.60	9.68
1004 – 1 (F)	3.10	25.47	1.63	3.35	20.90	21.59	13.61	4.17
1004 – 2 (F)	2.85	23.45	0.77	1.58	18.77	19.39	81.01	24.80
1004 – 3 (P)	---***	---***	---***	---***	---***	---***	---***	---***
1004 – 4 (F)	3.98	32.71	2.59	5.31	15.11	15.61	17.47	5.35
1004 – 5 (P)	4.21	34.61	3.39	6.97	15.18	15.68	44.90	13.75
1004 – 6 (P)	3.89	31.95	1.82	3.74	16.31	16.85	60.08	18.39
1004 – ave.	3.01	24.70	1.70	3.49	14.38	14.86	36.18	11.08
1005 – 1 (P)	5.72	46.98	2.35	4.83	18.54	19.15	10.70	3.28
1005 – 2 (P)	8.14	66.90	3.85	7.90	25.98	26.84	17.20	5.27
1005 – 3 (F)	10.49	86.16	3.35	6.87	27.05	27.94	11.61	3.55
1005 – 4 (P)	11.22	92.15	0.86	1.78	31.35	32.38	44.94	13.76
1005 – ave.	8.89	73.05	2.60	5.35	25.73	26.58	21.11	6.46
ALL – ave.	4.73	38.89	3.70	7.61	18.64	19.26	35.86	10.98

* Note: all milli-inch-pound/RPM^2 values shown are 10^5 times actual values for tabulation clarity.

** Note: a physical interpretation/meaning of Equivalent Geometry Error (EGE) for radial moments is vague.
*** Note: abbreviated test series obtained only axial and radial force IV data; no radial moment data

Table A-5: Computed EGE Coefficients for All Detected IV Radial Force Harmonic Ratios

Harm. Ratio↓ RWA ⟶	1001	1002	1003	1004	1005	Ave.
0.35	1.67**	1.70**	1.83**	1.20**	1.63**	1.61
1.00	8.84**	7.19**	12.67**	4.65**	16.16**	9.38
2.00	4.96**	4.07**	7.98**	4.01**	4.66**	4.94
2.82	11.72**	6.58**	9.29**	9.15**	15.53**	10.58
3.00	1.16*	--	1.39	2.07	1.49	1.53
3.12	2.27*	--	2.23	1.31	1.70	1.88
3.25	3.84*	--	2.98	1.62	4.74	3.30
3.60	1.81*	--	1.95	0.59	1.49	1.46
3.84	4.47*	--	5.13	1.14	6.31	4.26
4.00	2.86*	--	1.77	2.69	2.95	2.57
4.14	8.33**	6.37**	8.10**	3.91**	5.64**	6.47
4.55	5.26*	--	3.54	1.05	3.07	3.03
4.74	3.61*	--	3.63	1.39	3.07	2.93
5.00	2.85*	--	1.95	0.93	1.75	1.87
5.18	7.29**	6.48**	3.69**	3.71**	6.18**	5.34
5.60	14.39**	8.46**	5.99**	7.49**	13.71**	10.00
5.76	3.16*	--	2.01	2.51	14.50	5.55
6.00	16.05*	--	13.50	12.20	13.80	13.89
7.50	10.37**	7.26**	7.67**	3.48**	3.27**	6.41
8.28	11.45*	--	5.32	11.90	7.72	9.10
8.50	12.04**	10.01**	11.96**	11.49**	8.00**	10.70
8.70	--	--	--	--	11.80	11.80
9.00	10.90*	--	1.04	4.00	14.00	7.49
10.20	--	--	--	6.59	10.50	8.54
10.44	8.13*	--	7.01	4.85	10.10	7.52
10.80	7.22*	--	8.07	3.34	17.10	8.93
11.22	18.25*	--	22.00	19.30	29.50	22.26
11.88	13.80*	--	18.10	11.70	27.70	17.83

Note: all values shown are 10^6 times actual computed values.

Note: underlined plus bold items are 4 key harmonic ratios; underlined-only are next 4 secondary ratios.

-- Harmonic ratio value is below reliable detectability for this RWA's IV data.

* Average value for 2 data sets for this particular RWA.

** Average value for all data sets for this particular RWA.

Appendix B. Consolidated Validity Evaluations for RWA IV Datasets for Orbital IV Values

The CMG program data has several specific attributes as well as *deficiencies* listed below:
1) it measured effects (spin-axis reorientations) with established bases in HST RWA IV data,
2) it is a large enough body of data to provide valid statistical insights (where available and relevant for the specific effect being addressed), and
3) it is similar enough to the HST RWA design and contemporaneous configuration to provide applicable or extrapolate-able data and/or insights.

1) it does not directly address all variation effects sought,
2) it only measures effects on the radial direction 1.0 harmonic (i.e., unbalance/asymmetry) so inferences are needed for estimating effects on other harmonics and directions,
3) CMG program is classified, so it is limits access to analyze in a more detailed quantitative fashion data directly obtained; therefore, reliance turns towards supplier expertise and overall extrapolated guidelines from that database, and
4) CMG is not purely identical to the HST RWA design/configuration, creating some added uncertainty for full validity of applying extrapolations and engineering judgments.

The high value for accumulated CMG program data is to allow assessment of dataset variation due to:
1) change in spin-axis orientation in a 1-g gravitational field,
2) change from 1-g ambient to 0-g (or microgravity) orbital force field,
3) change from 1-atmosphere ambient to vacuum external-internal housing pressures, and
4) change from 70 deg F ambient to 50-90 degree F orbital operating temperatures.
Although the CMG data collected is the most relevant data available, it has noted constraints/caveats for directly-applicable data sought due to gaps in some key areas (i.e., no higher-ratio harmonics).

A) HST RWA Acceptance Test Procedure (ATP) IV test dataset collection is most directly applicable to the issue (i.e., design similarity), possessing the following attributes to allow investigating variabilities/causes:
1) it is precisely measured data on flight configured and realistically-tested RWAs,
2) it is a relatively large consistently-controlled sampling, implying decent statistical validity, and
3) it manifests negligible influence from some effects which alter IV output (e.g., wide swings in temperature or stress distribution changes during the test intervals).

It also has the following specific *deficiencies*:
1) each RWA is subjected to environmental exposures (random vibration or thermal-vacuum tests) between IV tests, so different dataset curve values solely due to fundamental IV test-to-test variations cannot be separately accounted for, and
2) amount of datasets for each RWA (3-4 typically, a lone exception being 6 on RWA 1004), is not sufficiently large for very high statistical significance if scatter is large (sometimes occurred).

The predominant value for IV test data collected is to provide the assessment basis for variations due to:
1) inherent RWA-to-RWA unit variation (i.e., determining which RWA will generally produce more or less jitter relative to another or the average, and how different the jitter variation would be),
2) test-to-test variations caused by inherent randomness and/or test setup/method limitations, and
3) test-to-test variations caused by exposure to environmental test conditions (i.e., Random Vibration and Thermal-Vacuum) plus inter-test handling/transport (believed to be much less significant).
The major restriction to more effective use of this body of data for more precise evaluation is that there is no definitive method for separating the last two effects: no data has been taken on an RWA without having both effects present; data scatter from both effects is notable.